RM E53F19

NACA

RESEARCH MEMORANDUM

MEASUREMENT AND ANALYSIS OF TURBULENT FLOW CONTAINING PERIODIC FLOW FLUCTUATIONS

By William R. Mickelsen and James C. Laurence

Lewis Flight Propulsion Laboratory
Cleveland, Ohio

NATIONAL ADVISORY COMMITTEE
FOR AERONAUTICS
WASHINGTON

August 19, 1953

NATIONAL ADVISORY COMMITTEE FOR AERONAUTICS

RESEARCH MEMORANDUM

MEASUREMENT AND ANALYSIS OF TURBULENT FLOW CONTAINING PERIODIC FLOW FLUCTUATIONS

By William R. Mickelsen and James C. Laurence

SUMMARY

Techniques are presented for the measurement of the energy spectrum of flow fluctuations in both axial and lateral flow directions. A simple spectrum analysis is presented by which quantitative distinction may be made between turbulence and the flow disturbances associated with sound waves in ducts. Experimental data are presented which indicate that the energy spectrum of the turbulence is not affected by periodic and random sound disturbances outside the frequency ranges containing the disturbances. Preliminary measurements are presented that illustrate the effect of combustion on the approach-stream velocity-fluctuation spectra in a ram-jet combustor.

INTRODUCTION

To date, major emphasis has been placed on the measurement of steady-state flow parameters in jet-engine combustor approach air streams and in various fundamental test installations, while the measurement of instantaneous mass-flow fluctuations has been largely ignored. However, problems recently encountered in the development of full-scale jet engines indicate that fluctuations of the mass air flow may strongly influence the diffusion of mass, heat, and momentum. In addition, anomalous results obtained from various fundamental research programs indicate that flow fluctuations seriously affect the mechanism under study.

It is therefore of immediate interest to investigate and to develop suitable techniques for the measurement and analysis of flow fields of the type encountered in jet engines. The purpose of this program was fourfold:

1. To adapt instrumentation for the measurement of the instantaneous flow fluctuations in both axial and lateral flow directions and for the resolution of these measurements into kinetic energy spectra

2. To measure the instantaneous flow fields of several distinctly different types of test apparatus and to develop techniques for the interpretation of the spectral forms obtained from such measurements

3. To determine the effect of periodic and random flow disturbances on the normal turbulence spectrum

4. To make a preliminary investigation of the effect of combustion on the approach flow field in a ram-jet combustor

A turbulent flow field containing periodic flow fluctuations was investigated in a small-scale wind tunnel used for fundamental combustion research. Additional measurements were made in a specially constructed duct where the frequency and magnitude of the periodic mass-flow disturbances could be controlled. A preliminary investigation of the combustor approach flow field was conducted in a connected-pipe ram-jet test installation under both burning and nonburning conditions. The instantaneous measurements of the mass-flow fluctuations (which may contain both turbulence and sound fluctuations) were made with constant-temperature hot-wire anemometer equipment, the basic components of which are described in reference 1. Instantaneous pressure fluctuations associated with the sound disturbances were measured with a standard microphone.

The investigations were carried out at the NACA Lewis laboratory as a part of the jet-engine combustion research program.

SYMBOLS

The following symbols are used in this report:

A	constant in King's equation
a	local speed of sound
B	constant in King's equation
C	calibration constant of hot-wire probes
e	voltage drop across hot wire
ΔE	direct-current potential difference between two hot-wire bridges
$\overline{E^2}$	mean-square voltage signal after amplification
$F(n)$	longitudinal or axial spectrum energy-density function

f	Kármán-Howarth correlation coefficient
$G(n)$	lateral spectrum energy-density function
g	Kármán-Howarth correlation coefficient
i	current
K	gain (amplification)
L_x	longitudinal scale of turbulence
M	local Mach number
n	frequency
p	static pressure
q	particle velocity in sound wave
R	resistance (electrical)
$\mathscr{R}$	correlation coefficient
T	temperature
U	free-stream mean velocity
u,v,w	velocity fluctuations in x-, y-, and z-directions, respectively
x,y,z	rectangular coordinates with x in direction of free-stream velocity U
α	temperature coefficient of resistance
β	power-band width of wave analyzer
$\delta_i(n-n_i)$	Dirac delta functions
θ	angle between sound wave and x-axis
ρ	density of air stream
φ	angular position of X-wire array

Subscripts:

a	ambient condition
b	difference
c	continuous portion of spectrum
i=1,2,...m	conditions at discrete or particular frequencies or at different stations x
r	resultant
s	sound fluctuations
t	turbulent fluctuations
u	longitudinal component of velocity fluctuations
v	lateral component of velocity fluctuations
x	longitudinal (x) direction
0	no-flow condition

Barred symbols indicate a time average

THEORETICAL CONSIDERATIONS

Spectrum of Turbulence

A turbulent field may be described by several parameters, of which the spectrum seemed the most appropriate for this investigation. The spectrum of turbulence, as defined by Taylor in reference 2, is the frequency distribution of the kinetic energy contained in the fluctuating velocity components of a turbulent fluid stream. For a unit mass of fluid, the total kinetic energy $\overline{u^2}$ contained in the longitudinal velocity fluctuations is the sum of the contributions $\overline{u^2}F(n)\,dn$ contained in the frequency intervals n to $n + dn$, over the range of n from zero to infinity. The energy-spectrum density function $F(n)$ satisfies the condition $\int_0^\infty F(n)\,dn = 1$. If a turbulent field having a range of eddy sizes flows past a stationary point, then the low-frequency portion of the spectrum measured at that point roughly represents the kinetic energy contained in the large eddies, and the high-frequency portion roughly represents the kinetic energy contained in the small eddies.

Taylor shows that, if the turbulent field moves past the point of measurement at the mean stream velocity, the spectrum density function is the Fourier transform of the longitudinal correlation coefficient $\mathscr{R}_x$:

$$F(n) = \frac{4}{U} \int_0^\infty \mathscr{R}_x \cos \frac{2\pi n x}{U} \, dx \tag{1}$$

where

$$\mathscr{R}_x = \frac{\overline{u_{x,1} u_{x,2}}}{\overline{u^2}} \tag{2}$$

Dryden notes (ref. 3) that experimentally measured correlation coefficients are usually exponential in form and suggests that $\mathscr{R}_x$ be represented by

$$\mathscr{R}_x = e^{-x/L_x} \tag{3}$$

where L_x is called the longitudinal scale of turbulence and is defined as

$$L_x = \int_0^\infty \mathscr{R}_x \, dx \tag{4}$$

If the $\mathscr{R}_x$ defined by equation (3) is substituted into equation (1), then the spectrum density function becomes

$$F(n) = \frac{\frac{4L_x}{U}}{1 + \left(\frac{2\pi L_x}{U}\right)^2 n^2} \tag{5}$$

The longitudinal spectrum density function as given by equation (5) is shown in figure 1(a) for a mean stream velocity U of 200 feet per second and for various values of L_x. Experimentally measured spectra in various air streams indicate that equation (5) may be taken as a characteristic form of the longitudinal turbulence spectrum (refs. 3, 4, and 5).

If a turbulent field has a longitudinal spectrum of the form defined by equation (5), and if the turbulent field is isotropic, then the lateral spectrum density function has the following form:

$$G(n) = \frac{2L_x}{U}\left\{\frac{1 + 3\left(\frac{2\pi L_x}{U}\right)^2 n^2}{\left[1 + \left(\frac{2\pi L_x}{U}\right)^2 n^2\right]^2}\right\} \tag{6}$$

The derivation of equation (6) is given in appendix A. The lateral spectrum density function as given by equation (6) is shown in figure 1(b) for a mean stream velocity of 200 feet per second and for various values of L_x.

Spectrum of Turbulence with Discrete Periodicities

Because this investigation is concerned in part with turbulent fields having additional flow disturbances of a periodic nature, it is of interest to discuss the spectral form of such fields. If a velocity component u is considered to be composed of two parts, one due to the random fluctuations u_t of the turbulence and the other due to the random sound fluctuations u_s, then

$$u = u_t + u_s \tag{7}$$

Because a velocity-sensitive instrument, such as a hot-wire anemometer, cannot distinguish between the u_t and the u_s, the mean square of its velocity reading will be

$$\overline{u^2} = \overline{(u_t + u_s)^2} \tag{8}$$

Expansion of equation (8) results in

$$\overline{u^2} = \overline{u_t^2} + \overline{2u_t u_s} + \overline{u_s^2} \tag{9}$$

If the velocity correlation term $\overline{2u_t u_s}$ is zero, or negligible, then the turbulence and sound-energy spectra are directly additive. If periodic and random sound disturbances are present in addition to the turbulence, then the spectrum density function of the combined field may be represented in the manner shown in references 5 and 6:

$$F(n) = \frac{\overline{u_t^2}}{\overline{u^2}} F_t(n) + \frac{\overline{u_s^2}}{\overline{u^2}} F_s(n) + \frac{\overline{u_1^2}}{\overline{u^2}} \delta_1(n-n_1) + \frac{\overline{u_2^2}}{\overline{u^2}} \delta_2(n-n_2) + \cdots \tag{10}$$

where $\overline{u^2}$ represents the total kinetic energy of the field, $\overline{u_t^2}$ the kinetic energy of the turbulence, and $\overline{u_s^2}$ the kinetic energy of the random sound-velocity fluctuations. The terms $\overline{u_1^2}$, $\overline{u_2^2}$, . . . represent the kinetic energy contained in the periodic sound-velocity fluctuations at the frequencies n_1, n_2, . . . , and the $\delta_i(n-n_i)$ are Dirac delta functions that satisfy the condition $\int_{-\infty}^{\infty} \delta_i(n-n_i)\, dn = 1$ and that are zero everywhere except at the discrete frequencies n_i. A spectrum of the type described by equation (10) is shown in figure 2.

The parameters described in the preceding theoretical considerations form a basis for a concise and descriptive method of representing fluctuating flow fields such as are the subject of the present investigation. The total kinetic energy of the velocity-fluctuation field is characterized by the quantity $\overline{u^2}$, and the frequency distribution of the total kinetic energy is given by the spectrum density functions $F(n)$ and $G(n)$.

INSTRUMENTATION

Hot-Wire Anemometer

The apparatus used for the measurement of the instantaneous longitudinal and lateral mass-flow fluctuations is shown diagrammatically in figures 3(a) and (b), respectively. The bridge-amplifier combination was identical to the constant-temperature hot-wire equipment described in reference 1. In the sections Calibration of Single-Wire Probe and Calibration of X-Wire Probe, equations are presented that relate the hot-wire electrical signal to the stream-velocity fluctuations. These equations were derived with the assumption of incompressibility, and, as shown in appendix B, this assumption is valid for both turbulence and sound fluctuations when the stream Mach number is low.

Hot-Wire Probes

Two different hot-wire-probe configurations were used in this investigation (fig. 4). The single-wire probe was used for the measurement of the longitudinal velocity component. When placed perpendicular to the direction of the longitudinal velocity component, the single hot wire is relatively insensitive to components other than the longitudinal (ref. 7). The X-wire probe was used to measure the lateral components of the velocity fluctuations. Calibration of the two probes is discussed in the sections Calibration of Single-Wire Probe and Calibration of X-Wire Probe.

The sensitive element of both probes was 0.0002 inch in diameter and 0.10 inch in length tungsten wire having an unplated length of 0.080 inch. The tungsten wire was prepared for mounting on the probes by the copperplating technique described in reference 8.

The current leads from the hot-wire supports were separated by a ceramic insulator throughout the length of the probe body to reduce interconductor capacitive effects. The ends of the probes were fitted with cable connectors to facilitate installation.

Calibration of Single-Wire Probe

King's equation (ref. 9) represents the heat transfer from a cylinder to a fluid flowing in a direction perpendicular to the cylinder. In the notation used herein the equation is

$$\frac{i^2R}{R - R_a} = A + B\sqrt{\rho U} \tag{11}$$

For the constant-temperature hot-wire operation used in this investigation, equation (11) may be reduced to (ref. 1)

$$u = C_u e \tag{12}$$

where the sensitivity C_u is

$$C_u = \frac{4iU}{R(i^2 - i_0^2)} \tag{13}$$

(Equations (12) and (13) are also in the notation used herein.) From equations (12) and (13), it is evident that the mean stream velocity U, the hot-wire resistance R, and the wire currents i and i_0 must be known in order to evaluate C_u. Since the wire is kept at a constant temperature by the amplifier-bridge circuit, the resistance R of the hot wire remains essentially constant at the value of the opposing bridge resistor, with a small correction sometimes necessary because of the mean bridge unbalance, as described in reference 1. The hot-wire operating resistance R was determined from figure 5 for an average value of R_a.

The wire current i_0 was evaluated by operating the hot-wire probe in quiescent fluid, with the fluid at a temperature equal to the total temperature of the fluid stream at the test conditions. An error is

introduced by this procedure, because equation (11) does not account for heat loss to the wire supports or for natural convection. However, this error is small for the range of mass velocities usually encountered in jet-engine research. When the test stream was above room temperature, a small quantity of the heated air was drawn off into an insulated chamber containing the probe so that i_0 could be evaluated at the stream total temperature.

The operating wire current i was measured with the probe in position and with the stream at the operating conditions. Correction for the division of bridge current was necessary; for greater accuracy, the bridge current was measured with a potentiometer connected across a precision 1-ohm resistor (fig. 3(a)).

Calibration of X-Wire Probe

The X-wire probes were calibrated by the method described in reference 7. The sensitivity of the X-wire array to the lateral velocity component was found by measuring the direct-current voltage difference ΔE between the two bridges (fig. 3(b)) for various angular positions φ of the probe at the stream operating conditions. From a graph of ΔE against φ, the sensitivity of the probe to the lateral component of the velocity fluctuations was obtained from the relation

$$C_v = \frac{2U}{\left(\frac{d\Delta E}{d\varphi}\right)_{\Delta E=0}} \tag{14}$$

where the slope of the calibration curve has the units volts per radian, and the numerical constant 2 is due to the voltage division across the bridge. A typical plot of ΔE against φ is shown in figure 6. The sensitivity C_v relates the lateral velocity component to the signal voltage through the expression

$$v = C_v e_b \tag{15}$$

where the signal voltage e_b is the instantaneous alternating-current voltage difference between the two hot wires in the X-array.

Measurement of Longitudinal Velocity Fluctuations

The root-mean-square value of the longitudinal velocity fluctuations was determined from the relation

$$\sqrt{\overline{u^2}} = \frac{C_u}{K}\sqrt{\overline{E^2}} \tag{16}$$

where the voltage $\sqrt{\overline{E^2}}$ was measured with an electronic average-square computer as described in reference 1. The gain K includes the amplification of the hot-wire voltage e by both the decade amplifier and the bridge-voltage division, since the signal voltage is measured across the entire bridge as shown in figure 3(a).

In the absence of discrete periodicities close to the frequency n, the longitudinal spectrum density function at the frequency n was determined from the relation:

$$F(n) = \frac{\overline{E_n^2}}{\beta\,\overline{E^2}} \tag{17}$$

where $\overline{E_n^2}$ is the square of the wave-analyzer voltage reading with the wave-analyzer frequency dial set at the frequency n, and $\overline{E^2}$ is the square of the average-square computer reading. Since the response of the wave analyzer was essentially constant over its narrow band width, an effective power-band width was used; therefore, β in equation (17) was equal to 5 cycles per second.

Since the analyzer made no distinction between the continuous spectra and discrete periodicities lying within its band width, another equation was required for such cases. It was assumed that the periodic velocity fluctuations were additive, so that the spectrum density in continuous portions of the spectrum immediately adjacent to the band containing the periodicity could be subtracted from the value indicated by the wave analyzer and thereby give the value of the spectral contribution of the discrete periodicity:

$$\frac{\overline{u_1^2}}{\overline{u^2}}\,\delta_1(n-n_1) = \frac{\overline{E_{n,1}^2} - \overline{E_c^2}}{\overline{E^2}} \tag{18}$$

where $\overline{E_{n,1}^2}$ is the square of the wave-analyzer voltage reading at the frequency n_1, $\overline{E_c^2}$ is the square of the wave-analyzer reading at a frequency adjacent to the band width containing n_1, and $\overline{E^2}$ was the square of the voltage reading of the average-square computer.

Measurement of Lateral Velocity Fluctuations

The total root-mean-square value and the mean-square values at particular frequencies of the lateral velocity fluctuations were determined from relations similar to those of the preceding paragraph. The total root-mean-square value was determined from:

$$\sqrt{\overline{v^2}} = \frac{C_v}{K}\sqrt{\overline{E_b^2}} \tag{19}$$

where the voltage $\sqrt{\overline{E_b^2}}$ was measured with the instantaneous-difference circuit and the average-square computer as shown in figure 3(b). The instantaneous-difference circuit is described in reference 1.

The lateral spectrum density function in the continuous portions of the spectrum was determined from the relation

$$G(n) = \frac{\overline{E_{b,n}^2}}{\beta\,\overline{E_b^2}} \tag{20}$$

where $\overline{E_{b,n}^2}$ is the square of the wave-analyzer reading at the frequency as shown in figure 3(b), and $\overline{E_b^2}$ is the square of the average-square-computer reading, also shown in figure 3(b). In the discontinuous portions of the lateral spectrum, the following expression was employed:

$$\frac{\overline{v_1^2}}{\overline{v^2}}\,\delta_1(n-n_1) = \frac{\overline{E_{b,n,1}^2} - \overline{E_{b,c}^2}}{\overline{E_b^2}} \tag{21}$$

where the derivation and symbols are similar to those of equation (18).

Measurement of Sound-Pressure Fluctuations

A microphone with matching power supply and preamplifier was used to measure the magnitude of the sound-pressure fluctuations for comparison with the hot-wire-anemometer measurements. The microphone-output voltage was analyzed with the average-square computer and the wave analyzer in a manner similar to that used for the hot-wire-output voltage. The theoretical sound-pressure - velocity relation (ref. 10, p. 158) was employed to convert the microphone-output voltage to values of the fluctuation velocity associated with the pressure fluctuations. The low-frequency response of the microphone was determined by comparison in a loud-speaker sound field with a reference microphone that had been previously calibrated by a reciprocity method.

APPARATUS

Small-Scale Wind Tunnel

The small-scale wind tunnel that was investigated in this program is shown in figure 7. This tunnel was being used for a spark-ignition investigation described in reference 11. Room air was drawn through the tunnel by means of the laboratory altitude-exhaust facility. The tunnel static pressure was held constant throughout the tests at a value of 5 inches of mercury absolute. The tunnel velocity was varied through a range from 50 to 250 feet per second. The hot-wire probe was installed at the positions shown in figure 7 with the hot wire on the tunnel center line. The random turbulent field was generated by interchangeable grids placed at the tunnel inlet.

Controlled-Perturbation Duct

A specially constructed apparatus (fig. 8) was used for fundamental study of a turbulent field with superimposed periodic and semiperiodic flow fluctuations. The duct consisted of an 8-inch-diameter steel pipe, with a flared entrance section, open to the room at the inlet end and connected to the laboratory altitude-exhaust facility at the other end. A number of instrumentation stations were provided along the duct, as shown in figure 8. Two slotted plates, one fixed and the other free, were installed at the exhaust end of the duct. When oscillated by the electromagnetic-vibration test unit, the free plate introduced mass-flow perturbations throughout the length of the duct by causing periodic changes in the exhaust area. The vibration test unit was driven by a 1500-watt amplifier that received a signal from either an audio oscillator or a random-noise generator. The random-noise signal was passed through a low- and a high-pass filter so that the random flow fluctuations could be controlled with regard to magnitude, band width, and position in the spectrum.

Mass velocities in the duct were determined with a standard pitot tube, wall static-pressure taps, and standard thermocouples.

Ram-Jet Installation

Measurements with the hot-wire-anemometer equipment were also made in the connected-pipe ram-jet test installation shown in figure 9. The hot-wire probes were placed on the duct center line at the station shown in figure 9. At this point in the duct, the test conditions were held constant at a velocity of 265 feet per second, a static pressure of 30 inches of mercury absolute, and a total temperature of 200° F. Mass

air-flow rates were measured with a standard variable-area orifice, local stream velocities with standard pitot tubes, and air temperatures with standard thermocouples. Heated air was drawn directly from the air stream into an insulated chamber until the air in the chamber reached the stream total temperature, so that the single hot-wire probe could be calibrated as described in the INSTRUMENTATION section.

RESULTS AND DISCUSSION

Measurement and Analysis of Turbulent-Flow Fields Containing Random and Periodic Flow Fluctuations

The present investigation was initiated during a turbulence survey of the small-scale wind tunnel that was incident to the spark-ignition program described in reference 11. Preliminary measurements in this tunnel indicated the presence of periodic flow disturbances in addition to the turbulence generated by the grids at the tunnel inlet. A typical measured longitudinal energy-density spectrum is shown in figure 10(a). The spectral positions of the discrete periodicities at 30, 850, and 1700 cycles per second were independent of tunnel velocity throughout the velocity range from 50 to 250 feet per second. Since the ducting length between the flow-control valves (V_1 and V_2 in fig. 7) and the exhaust choke was nearly that required for a closed-closed tube resonance of 30 cycles per second, it was concluded that the spectral discontinuity at that frequency was a standing sound wave. Similarly, it was concluded that the periodicities at 850 and 1700 cycles per second were the first and second harmonics of an open-open tube standing sound wave in the tunnel proper. These conclusions were strengthened by microphone measurements that qualitatively indicated periodic pressure fluctuations at these frequencies. Because of the low static pressure in the tunnel, the air-column to microphone-diaphragm coupling factor was unknown; therefore, the microphone-output voltage could not be converted to sound-perturbation velocity.

Comparison of the experimental spectrum shown in figure 10(a) with the reference spectrum shown in figure 1(a) indicates the presence of velocity fluctuations in the form of a continuous spectral distribution between 20 and 200 cycles per second in addition to the normal turbulence. Because it was suspected that these low-frequency spectral contributions might originate in the altitude-exhaust facility, several spectrum measurements were made at zero mass flow with direct coupling between the tunnel and the altitude-exhaust facility. The spectral form of these measurements is shown in figure 10(b), which, together with qualitative microphone sound-pressure measurements, indicates that the low-frequency continuous spectral contribution did originate in the exhaust facility.

From the preceding tests and observations, it was possible to divide the measured spectrum into three general regions: normal turbulence, periodic sound discontinuities, and random sound contributions. A typical experimental spectrum divided into these three regions is shown in figure 10(c). Comparison of figure 10(c) with figure 1(a) indicates that, aside from the spectral regions containing sound disturbances, the measured spectrum follows the reference spectral form based on the exponential correlation coefficient.

Upon completion of the spectral analysis outlined above, various mechanical changes were made in the ducting of the small-scale wind tunnel. Several unused branches of the piping were sealed off, and a more direct approach was provided for the entrance of room air into the ducting. In addition, the tunnel pressure was controlled with the valve V_3 instead of the valves V_1 and V_2 as shown in figure 7.

A comparison of the spectra measured before and after the mechanical revisions is shown in figure 11. It is evident from this comparison that the spectral portions attributed to turbulence were substantially unchanged by the elimination of the periodic and random sound disturbances. A typical spectrum measured after the ducting revisions (fig. 11(a)) is plotted in figure 12 over a family of reference spectrum curves generated from equation (5). From inspection of figure 12, the conformity of the measured spectrum to the theoretical reference spectrum can be observed. The longitudinal scale of the turbulence data shown in figure 12 was by inspection estimated to be 0.1+ inch. This value of the turbulence scale should be corrected for the effect of the hot-wire length as described in reference 12.

Effect of Random Sound Disturbances on Turbulence Spectrum

In order to determine the effect of sound on the turbulence spectrum, further investigation was carried out in the controlled-perturbation duct where quantitative measurements could be made with both the hot-wire anemometer and the microphone. The hot-wire probes were placed at the duct center line for all measurements, and the microphone was mounted so that the ports leading to the pressure-sensing element were 1/8 inch from the duct wall. Spectrum measurements were made at several mean stream velocities both with and without forced perturbations. A comparison between typical longitudinal spectrums with and without forced perturbations is shown in figure 13(a). It is evident from this figure that the spectrum is unchanged except in the region containing the forced perturbations. The spectrum in the lateral direction

was also measured, and a comparison between spectra with and without forced perturbations is shown in figure 13(b). This figure indicates that for the physical configuration of the duct and for the method of introducing the forced perturbations, the lateral spectrum was affected only slightly in the range of frequencies containing the forced perturbations.

The root-mean-square values of the sound-velocity fluctuations were determined from the microphone sound-pressure readings as described in the INSTRUMENTATION section, and their spectral distribution was determined with the wave analyzer. The spectral contributions of the forced perturbations, as measured with the microphone, were then added to the spectral values measured with no forced perturbations by means of equation (10). These calculated values of the spectrum density function are shown in figure 13(a); they indicate that the microphone readings approximately account for the spectral energy introduced by the forced perturbations. The maximum kinetic-energy contribution due to sound disturbances shown in figure 13(a) corresponds to a sound-pressure level of 122 decibels per cycle per second.

Effect of Combustion on Combustor Approach-Stream Spectrum

Typical longitudinal and lateral spectra measured in a ram-jet engine are shown in figures 14(a) and (b), respectively. The hot-wire probes were placed on the duct center line at the station shown in figure 9. The spectrum curves in figure 14(a) indicate that under stable combustion conditions, random fluctuations were superimposed on the normal longitudinal spectrum in the low-frequency range. A careful survey throughout the audio-frequency range revealed no other spectral contributions in the londitudinal direction. Comparison of figures 14(a) and (b) also indicates that the low-frequency contributions due to the presence of flame in the combustion zone existed only in the longitudinal direction. Figure 14(b) indicates the presence of periodic flow fluctuations in the lateral direction at fairly high frequencies for the nonburning condition. As mentioned previously, these high-frequency contributions did not appear in the longitudinal direction. Figure 14(b) also indicates that the presence of combustion did not greatly alter the lateral spectrum for the ram-jet operating condition investigated. While specific conclusions cannot be drawn from the preceding observations, it is apparent that the smooth spectral distribution characteristic of normal turbulence does not necessarily occur in connected-pipe ram-jet installations.

CONCLUSIONS

From the results of this investigation, the following conclusions may be drawn:

1. By use of the measurement and analytical techniques described in this report, random turbulent energy may be quantitatively distinguished from periodic and random sound disturbances in fluid streams.

2. The spectrum of combined turbulence and sound fields appears to be a simple superposition of their separate spectra without intermodulation for the range of sound intensities investigated, which included sound-pressure peaks up to 122 decibels per cycle per second.

3. In a preliminary investigation of a particular ram-jet combustor under conditions of smooth combustion, the axial energy spectrum of the approach stream was markedly affected by the combustion process. The lateral spectrum of the combustor approach stream contained high-frequency contributions of large magnitude that were not greatly affected by the combustion process.

Lewis Flight Propulsion Laboratory
National Advisory Committee for Aeronautics
Cleveland, Ohio, June 23, 1953

APPENDIX A

DERIVATION OF FORM OF LATERAL ISOTROPIC-TURBULENCE SPECTRUM BASED ON EXPONENTIAL FORM OF LONGITUDINAL CORRELATION COEFFICIENT

For isotropic turbulence, the relation between the Kármán-Howarth correlation coefficients f and g is (ref. 13):

$$2f + r\frac{\partial f}{\partial r} = 2g \tag{A1}$$

where f, g, and r are as shown in the following:

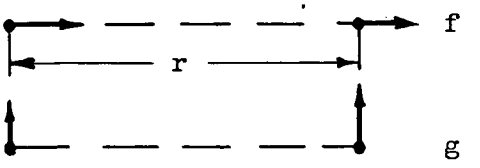

The correlation coefficient f corresponds to the $\mathscr{R}_x$ of equation (3), and r corresponds to x. Substitution of equation (3) into equation (A1) results in

$$2e^{-x/L_x} - x\left(\frac{1}{L_x}\right)e^{-x/L_x} = 2g \tag{A2}$$

so that

$$g = e^{-x/L_x}\left(1 - \frac{x}{2L_x}\right) \tag{A3}$$

In a manner analogous to that of equation (1), a Fourier transform may be employed to relate the lateral spectrum density function G(n) to the correlation coefficient g:

$$G(n) = \frac{4}{U}\int_0^\infty g \cos\frac{2\pi nx}{U}\,dx \tag{A4}$$

Substitution of equation (A3) into equation (A4) results in

$$G(n) = \frac{\frac{4L_x}{U}}{1 + \left(\frac{2\pi L_x}{U}\right)^2 n^2} - \frac{2L_x}{U} \frac{1 - \left(\frac{2\pi L_x}{U}\right)^2 n^2}{\left[1 + \left(\frac{2\pi L_x}{U}\right)^2 n^2\right]^2} \tag{A5}$$

which may be reduced to equation (6).

APPENDIX B

EFFECT OF DENSITY FLUCTUATIONS ASSOCIATED WITH SOUND FIELDS ON HOT-WIRE-ANEMOMETER RESPONSE

As noted in the INSTRUMENTATION section, the relations connecting the velocity fluctuations of the stream to the fluctuating voltage across the hot wire were based on the assumption that the instantaneous flow field was incompressible. It appears that this assumption is justified if the stream Mach number is relatively low. The following discussion is based upon an analysis by H. S. Ribner of the Lewis laboratory.

The hot-wire anemometer is sensitive to fluctuations in the mass velocity ρU, so that

$$e \propto \frac{d(\rho U)}{\rho U} \tag{B1}$$

Carrying out the differentiation,

$$\frac{d(\rho U)}{\rho U} = \frac{dU}{U} + \frac{d\rho}{\rho} \tag{B2}$$

which for small velocity fluctuations becomes

$$\frac{d(\rho U)}{\rho U} = \frac{u_t}{U} + \frac{u_s}{U} + \frac{(d\rho)_t}{\rho} + \frac{(d\rho)_s}{\rho} \tag{B3}$$

where u_t is the velocity-fluctuation component due to the turbulence, and u_s is the velocity fluctuation due to the sound field. Since the density fluctuations due to turbulence are negligible, equation (B3) may be written:

$$\overline{\left[\frac{d(\rho U)}{\rho U}\right]^2} = \frac{\overline{u_t^2}}{U^2} + 2\,\overline{\frac{u_t}{U}\left[\frac{u_s}{U} + \frac{(d\rho)_s}{\rho}\right]} + \overline{\left[\frac{u_s}{U} + \frac{(d\rho)_s}{\rho}\right]^2} \tag{B4}$$

If the turbulence and the sound disturbances have no correlation, which is a reasonable assumption, then the second term on the right side of equation (B4) becomes zero.

As shown in reference 10 (p. 48), the pressure fluctuation $(dp)_s$ in a sound wave is related to the particle velocity q by the equation

$$(dp)_s = \rho a q \tag{B5}$$

where a is the local speed of sound, and q is positive in the direction of propagation of the wave. The classical definition of the speed of sound is

$$a^2 = \left(\frac{dp}{d\rho}\right)_s \tag{B6}$$

and combining equations (B5) and (B6) results in

$$\frac{(d\rho)_s}{\rho} = \frac{q}{a} \tag{B7}$$

The sound-wave-particle velocity is related to the velocity component u_s by the expression

$$q = u_s \sec \theta \tag{B8}$$

where θ is the angular inclination of the sound wave to the x-axis.

By virtue of equations (B7) and (B8), the equation pertaining to a single wave is

$$\overline{\left[\frac{u_s}{U} + \frac{(d\rho)_s}{\rho}\right]^2} = \frac{\overline{u_s^2}}{U^2} + 2\,\frac{\overline{u_s\,(d\rho)_s}}{U\rho} + M^2\,\frac{\overline{q^2}}{U^2} \tag{B9}$$

When equation (B9) is applied to an array of sound waves, the term

$$2\,\frac{\overline{u_s\,(d\rho)_s}}{U\rho}$$

will average out to zero if the wave directions θ and $\pi-\theta$ are equally probable. For this type of symmetry, equation (B9) may be generalized as follows:

$$\overline{\left[\frac{u_s}{U} + \frac{(d\rho)_s}{\rho}\right]^2} = \frac{\overline{u_s^2}}{U^2} + M^2 \frac{\overline{q_r^2}}{U^2} \tag{B10}$$

where q_r is the particle velocity in a single wave that is equivalent to the array of sound waves. Combination of equation (B4) and the generalized equation (B10) results in

$$\overline{\left[\frac{d(\rho U)}{\rho U}\right]^2} = \frac{\overline{u_t^2}}{U^2} + \frac{\overline{u_s^2}}{U^2} + M^2 \frac{\overline{q_r^2}}{U^2} \tag{B11}$$

Since the Mach number M was low throughout the present investigation, then

$$\overline{\left[\frac{d(\rho U)}{\rho U}\right]^2} \cong \frac{\overline{u_t^2 + u_s^2}}{U^2} \tag{B12}$$

which is equivalent to the assumption of incompressibility, since from equation (B12)

$$\frac{d(\rho U)}{\rho U} \cong \frac{dU}{U} \tag{B13}$$

REFERENCES

1. Laurence, James C., and Landes, L. Gene: Auxiliary Equipment and Techniques for Adapting the Constant-Temperature Hot-Wire Anemometer to Specific Problems in Air-Flow Measurements. NACA TN 2843, 1952.

2. Taylor, G. I.: The Spectrum of Turbulence. Proc. Roy. Soc. (London), ser. A, vol. 164, Feb. 18, 1938, pp. 476-490.

3. Dryden, H. L.: A Review of the Statistical Theory of Turbulence. Quart. Appl. Math., vol. 1, no. 1, Apr. 1943, pp. 7-42.

4. Laufer, John: Investigation of Turbulent Flow in a Two-Dimensional Channel. NACA Rep. 1053, 1951. (Supersedes NACA TN 2123.)

5. Roshko, Anatol: On the Development of Turbulent Wakes from Vortex Streets. NACA TN 2913, 1953.

6. James, Hubert M., Nichols, Nathaniel B., and Phillips, Ralph S., eds.: Theory of Servomechanisms. First ed., McGraw-Hill Book Company, Inc., 1947.

7. Schubauer, G. B., and Klebanoff, P. S.: Theory and Application of Hot-Wire Instruments in the Investigation of Turbulent Boundary Layers. NACA WR-86, 1946. (Supersedes NACA ACR 5K27.)

8. Strehlow, Roger A.: A Method for Electroplating Fine Wires. Univ. Wisconsin, CM-551, June 27, 1949. (Navy BuOrd Contract Nord 9938, Task WIS-1-E.)

9. Lowell, Herman H.: Design and Applications of Hot-Wire Anemometers for Steady-State Measurements at Transsonic and Supersonic Airspeeds. NACA TN 2117, 1950.

10. Beranek, Leo L.: Acoustic Measurements. John Wiley & Sons, Inc., 1949.

11. Swett, Clyde C., Jr., and Donlon, Richard H.: Spark Ignition of Flowing Gases. III - Effect of Turbulence Promotor on Energy Required to Ignite a Propane-Air Mixture. NACA RM E52J28, 1953.

12. Dryden, Hugh L., Schubauer, G. B., Mock, W. C., Jr., and Skramstad, H. K.: Measurements of Intensity and Scale of Wind-Tunnel Turbulence and Their Relation to the Critical Reynolds Number of Spheres. NACA Rep. 581, 1937.

13. von Kármán, Theodore, and Howarth, Leslie: On the Statistical Theory of Isotropic Turbulence. Proc. Roy. Soc. (London), ser. A., vol. 164, no. 192, Jan. 21, 1938, pp. 192-215.

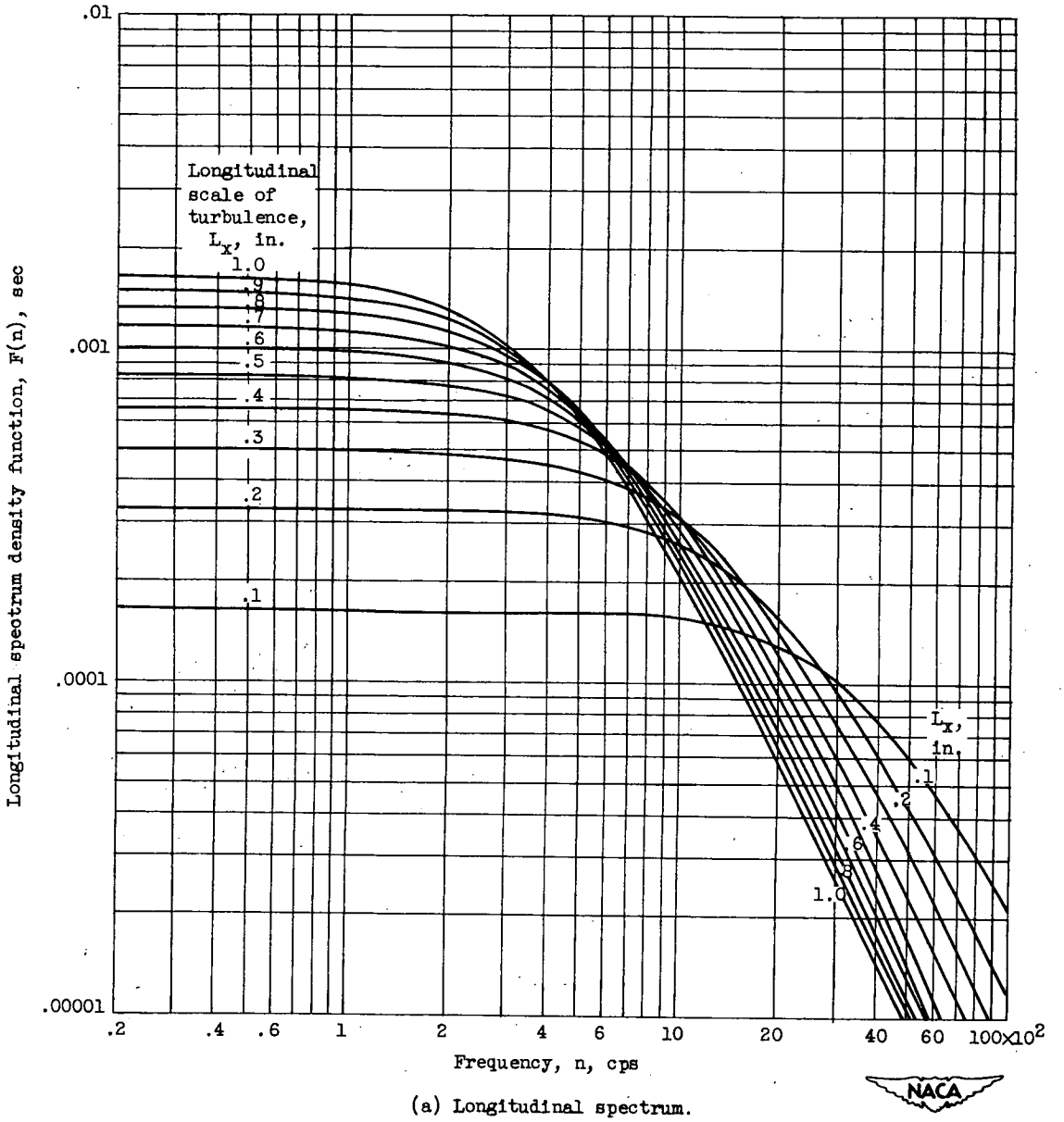

(a) Longitudinal spectrum.

Figure 1. - Spectra of turbulence for $\mathscr{R}_x = e^{-x/L_x}$ at mean stream velocity of 200 feet per second.

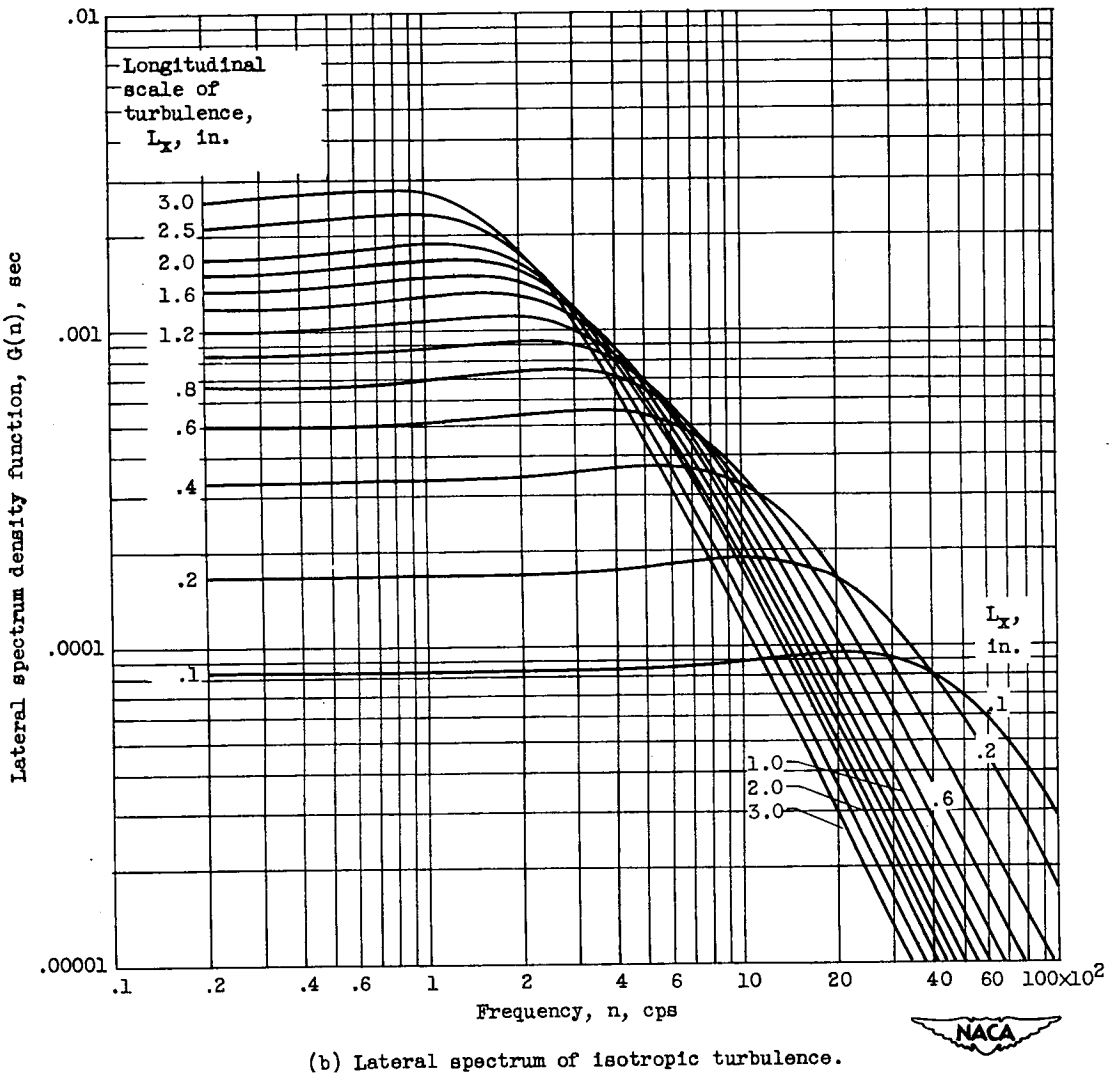

(b) Lateral spectrum of isotropic turbulence.

Figure 1. - Continued. Spectra of turbulence for $\mathscr{R}_x = e^{-x/L_x}$ at mean stream velocity of 200 feet per second.

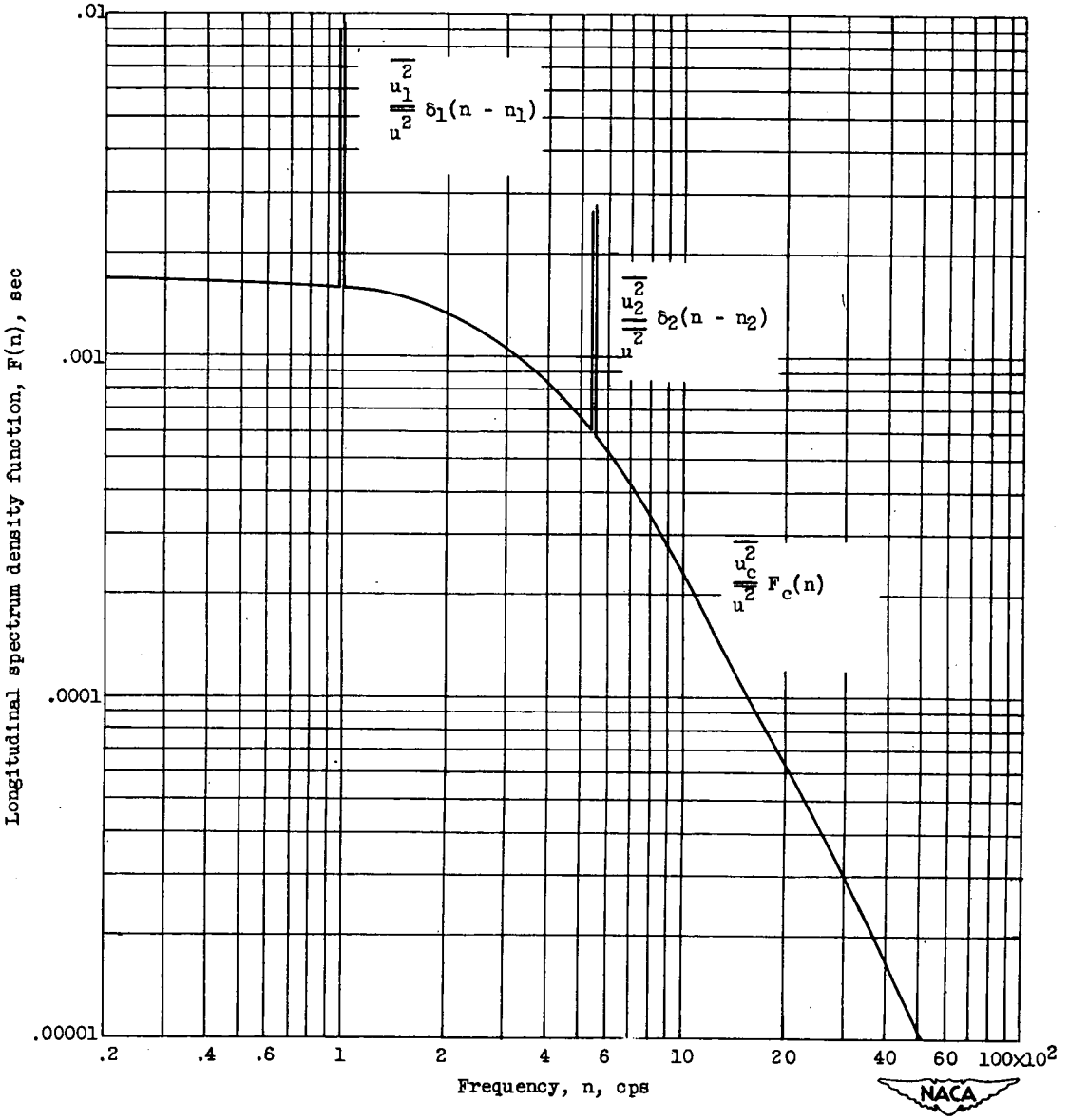

Figure 2. - Typical longitudinal spectrum containing discrete periodicities.

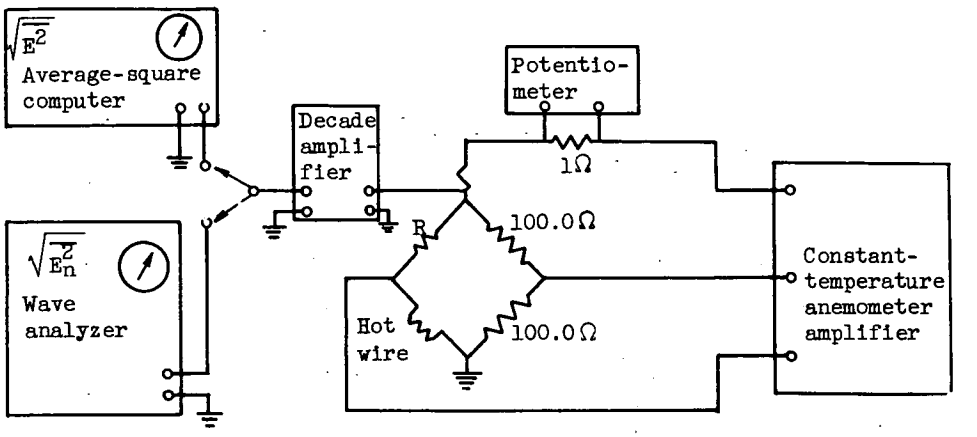

(a) Longitudinal fluctuations.

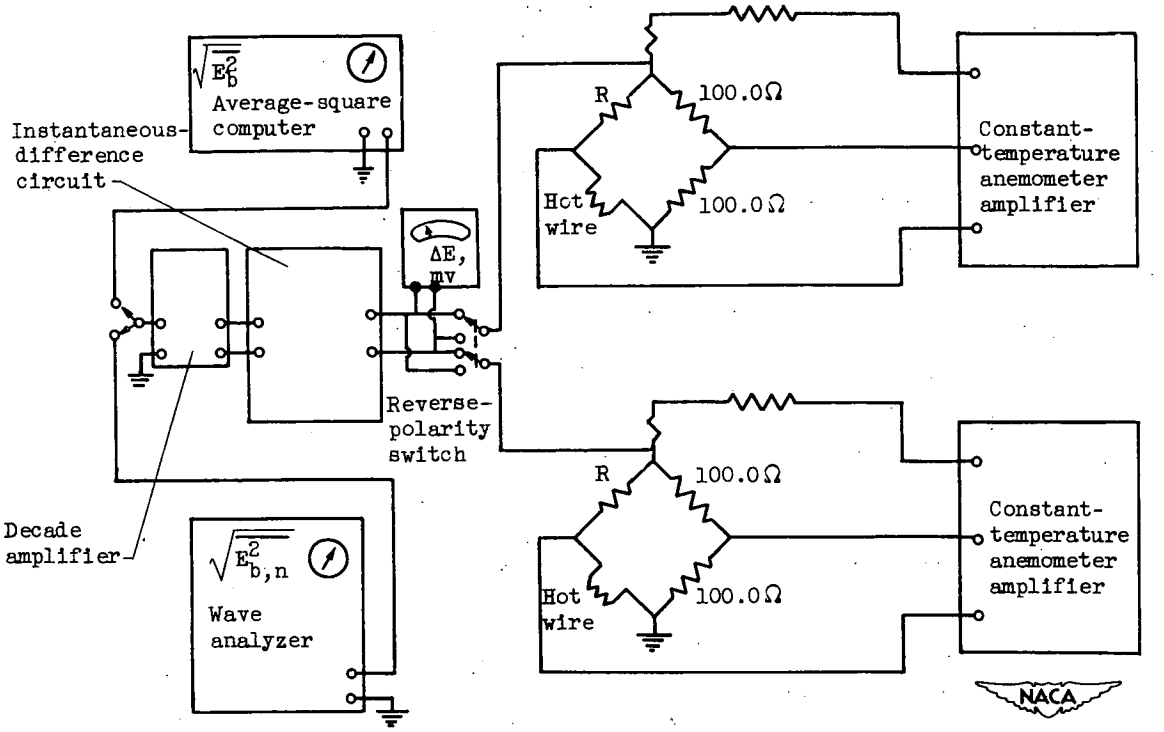

(b) Lateral fluctuations.

Figure 3. - Apparatus for measurement of longitudinal and lateral velocity fluctuations.

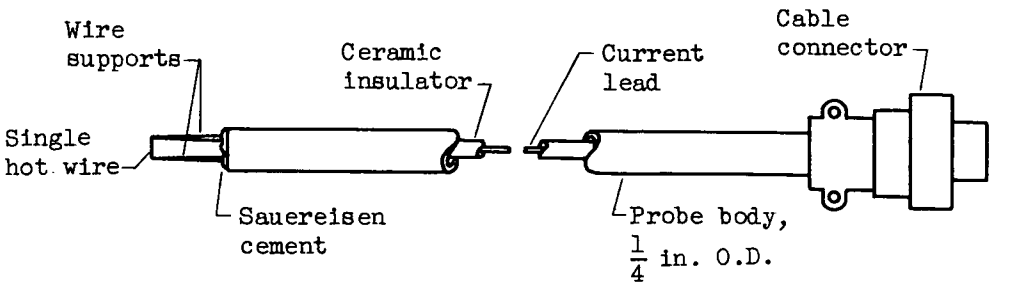

(a) Single-hot-wire probe.

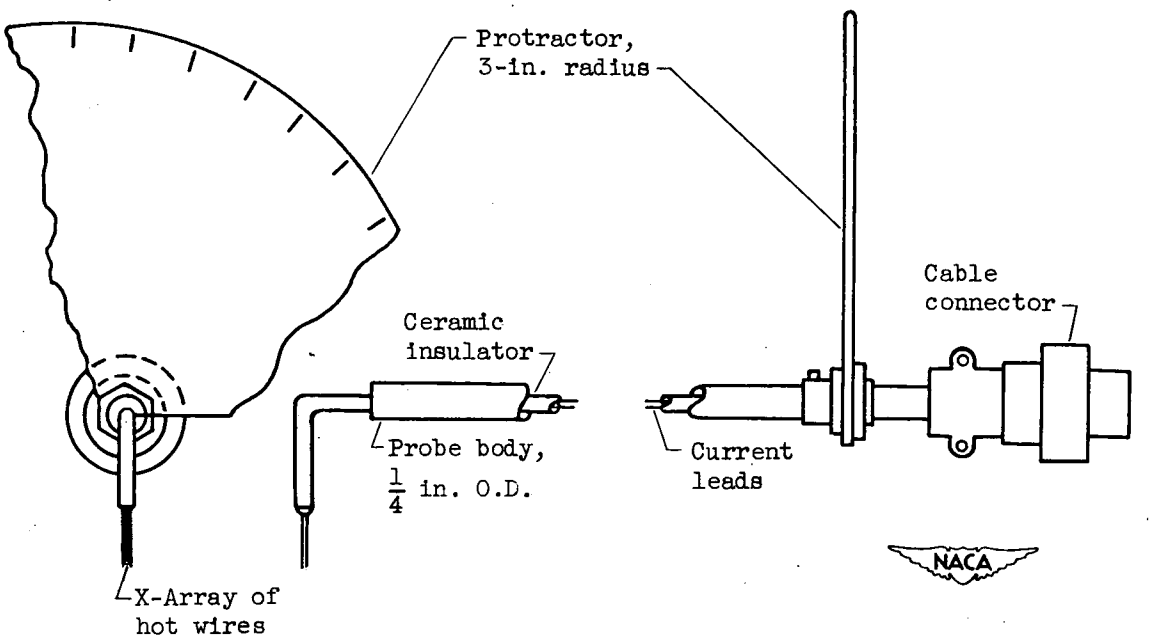

(b) X-wire probe.

Figure 4. - Hot-wire probes.

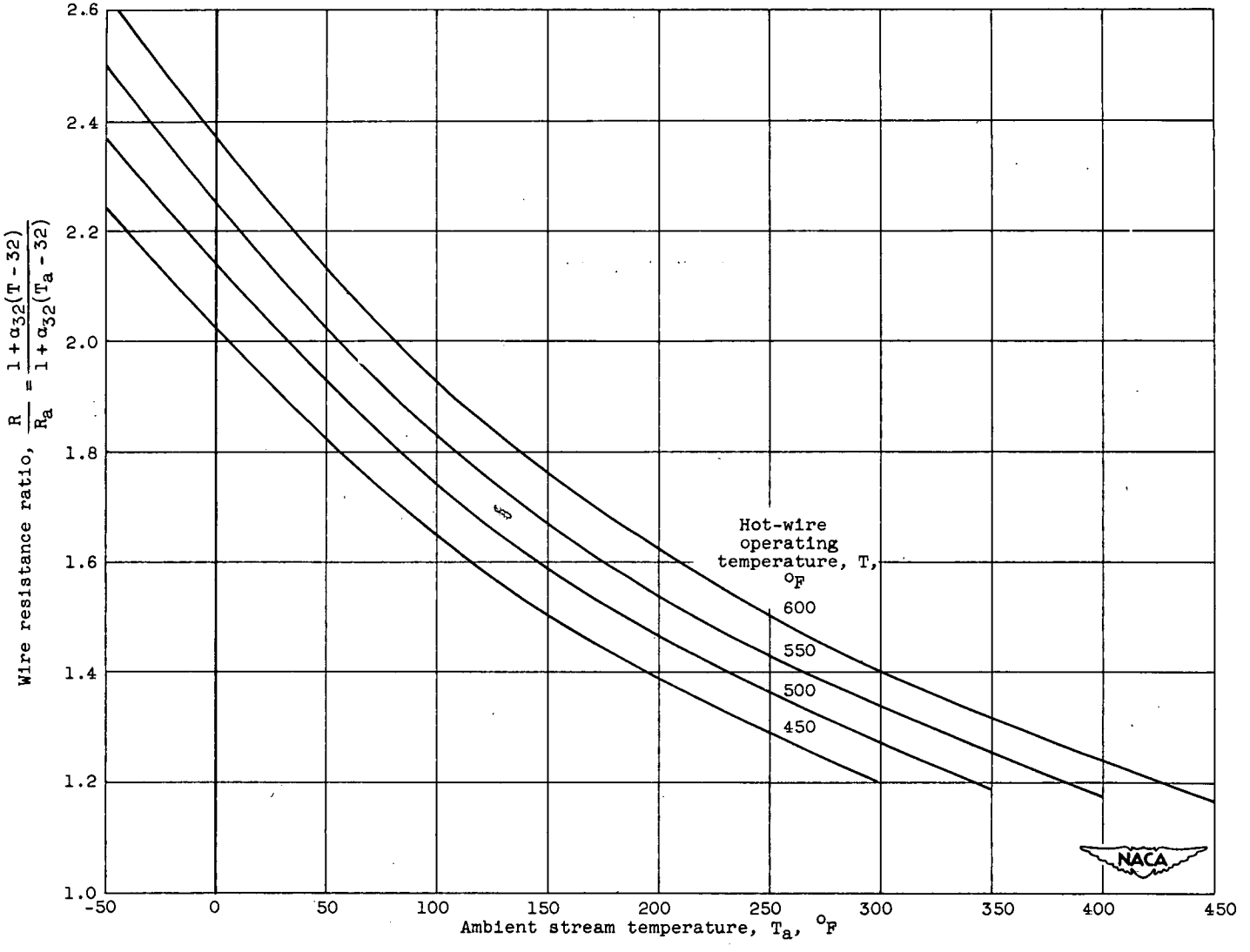

Figure 5. - Operating resistance for tungsten hot wires. Temperature coefficient of resistance, α_{32}, 0.00211 ohm/ohm °F. (Maximum safe operating temperature for tungsten ≈ 625° F.)

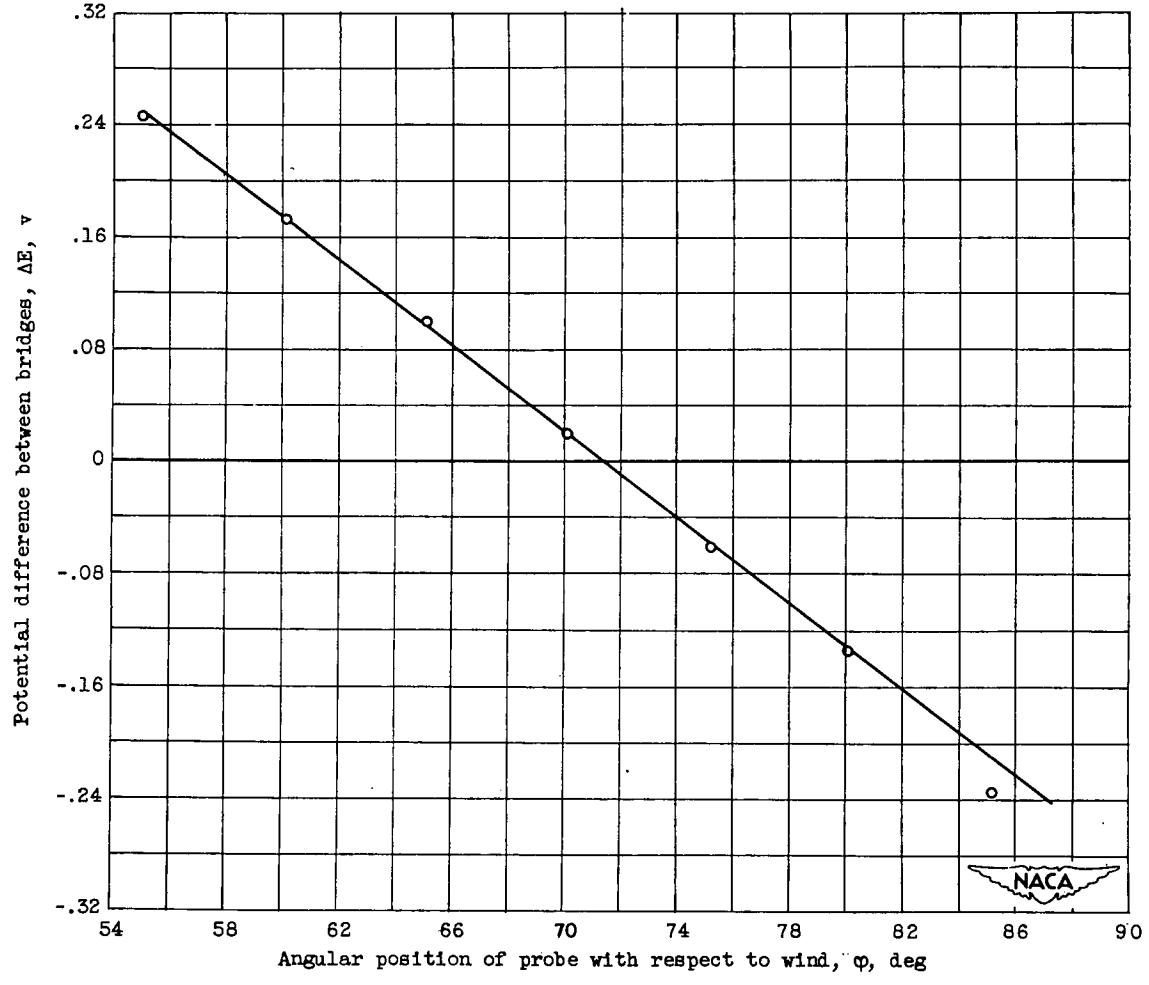

Figure 6. - Typical calibration curve for X-wire probe.

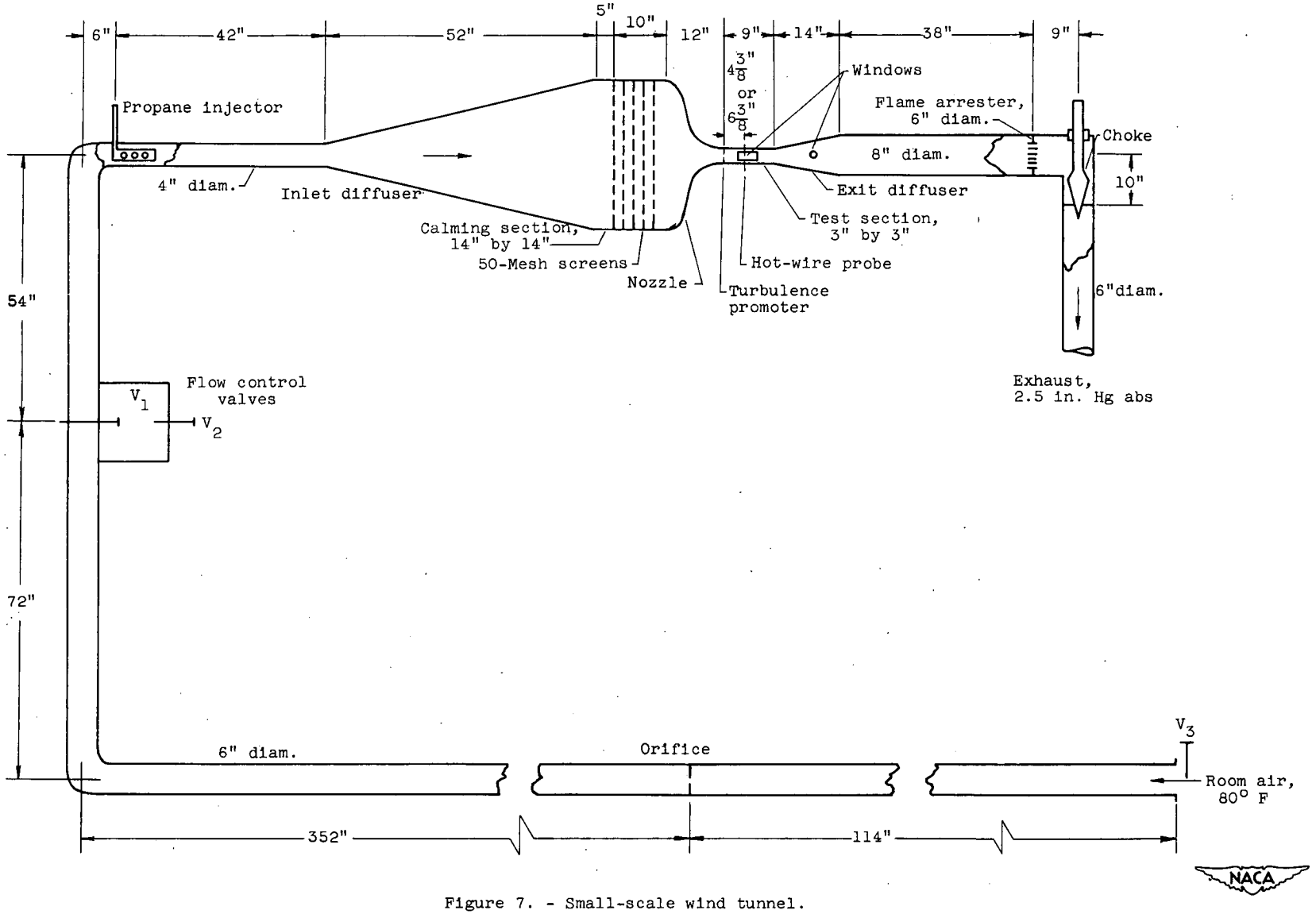

Figure 7. - Small-scale wind tunnel.

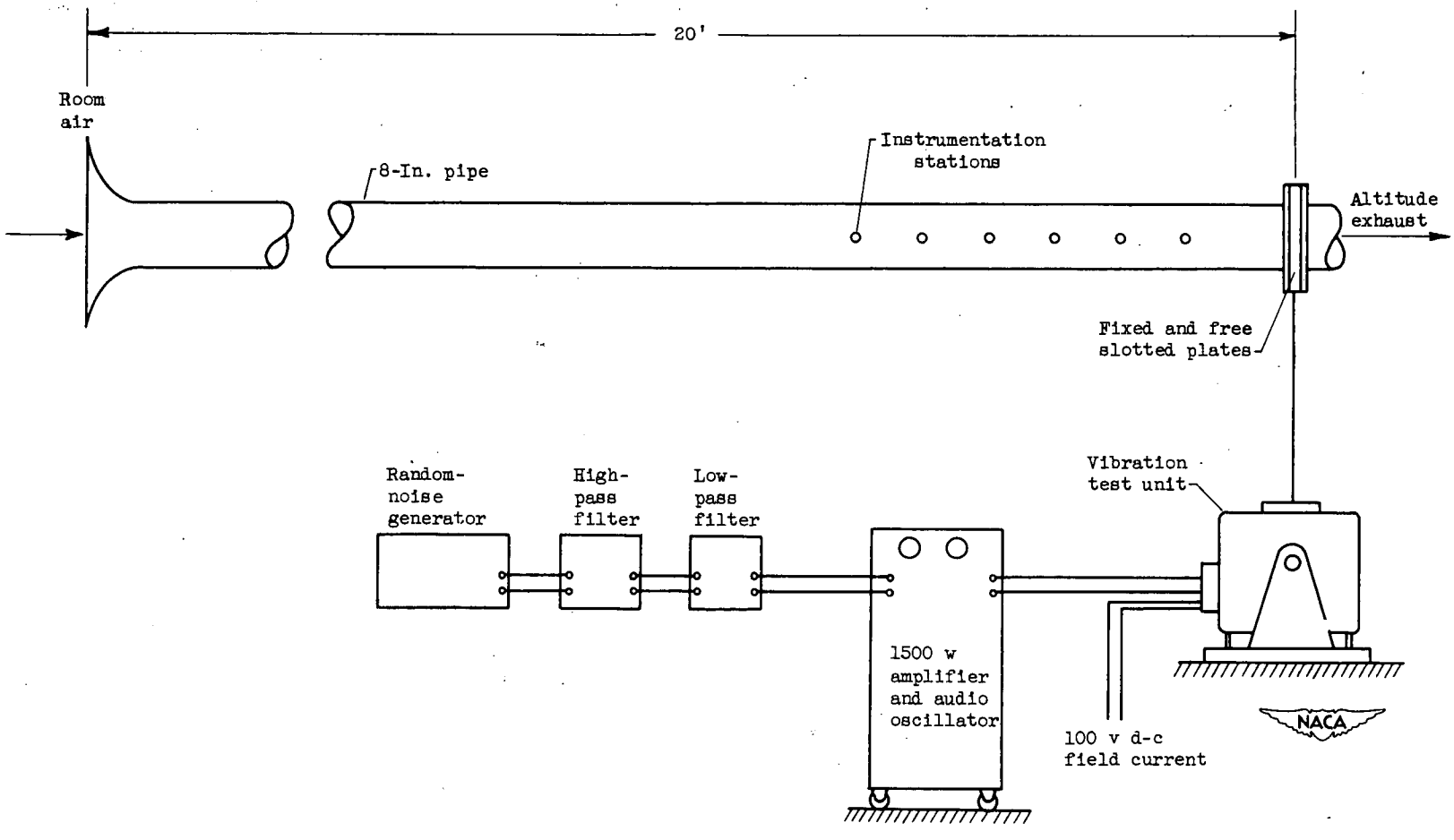

Figure 8. - Controlled-perturbation duct and auxiliary apparatus.

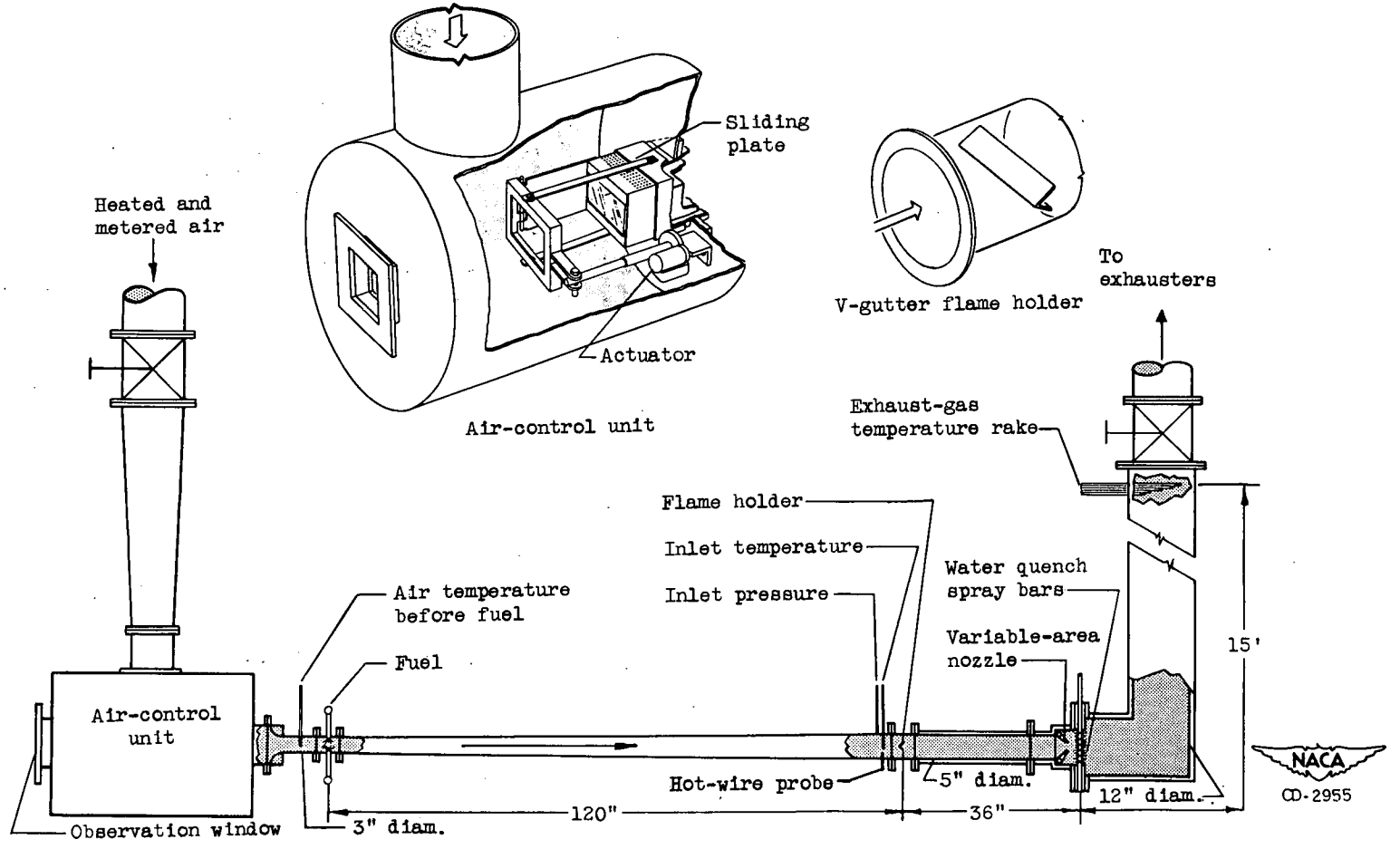

Figure 9. - Schematic illustration of 5-inch ram-jet combustor test installation, flame holder, and air-control unit.

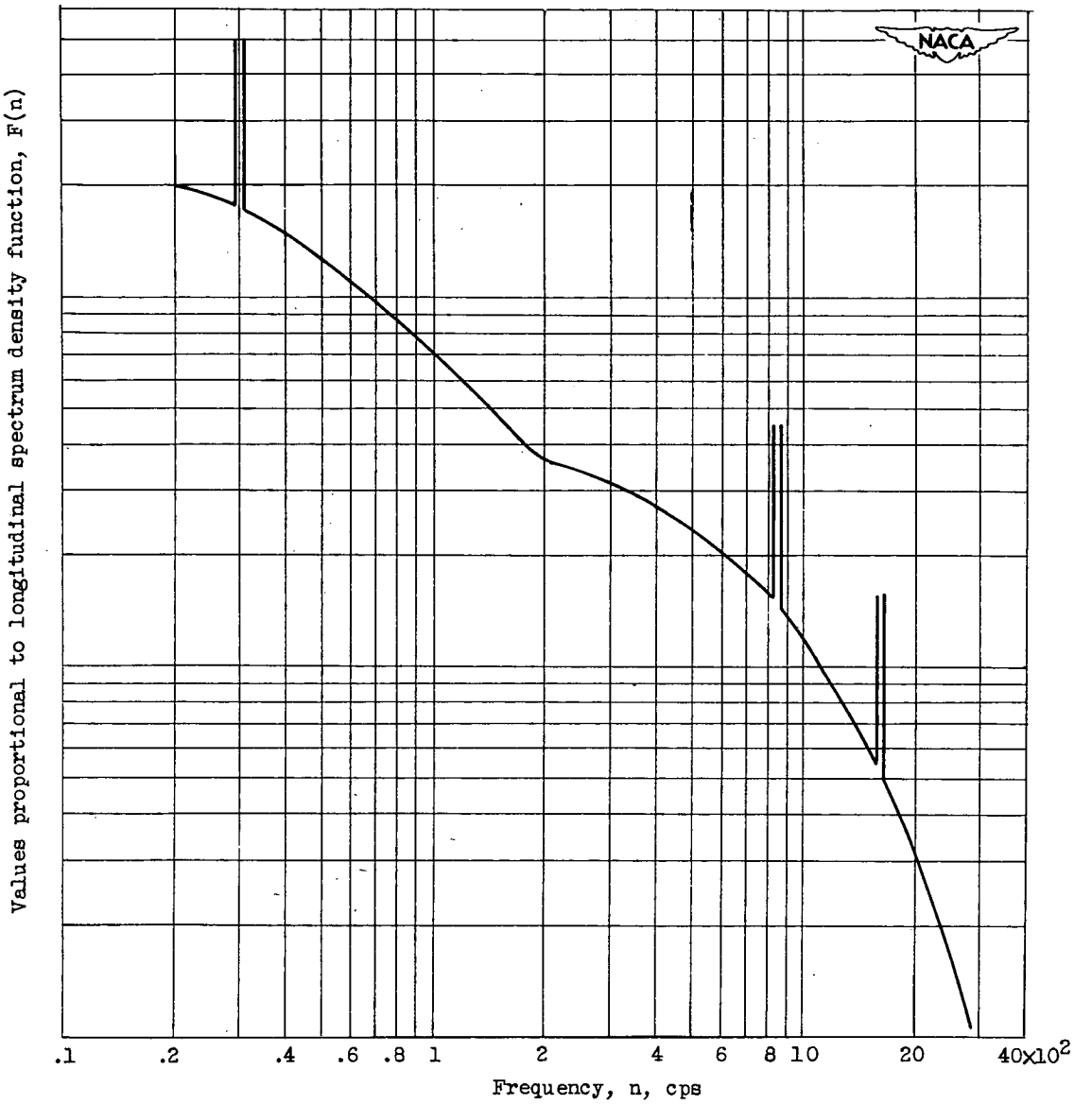

(a) Turbulence with superimposed exhaust pulsations and ducting resonance. Mean stream velocity, 50 feet per second; stream static pressure, 5 inches of mercury absolute; air temperature, 540° R.

Figure 10. - Measured longitudinal energy spectrum.

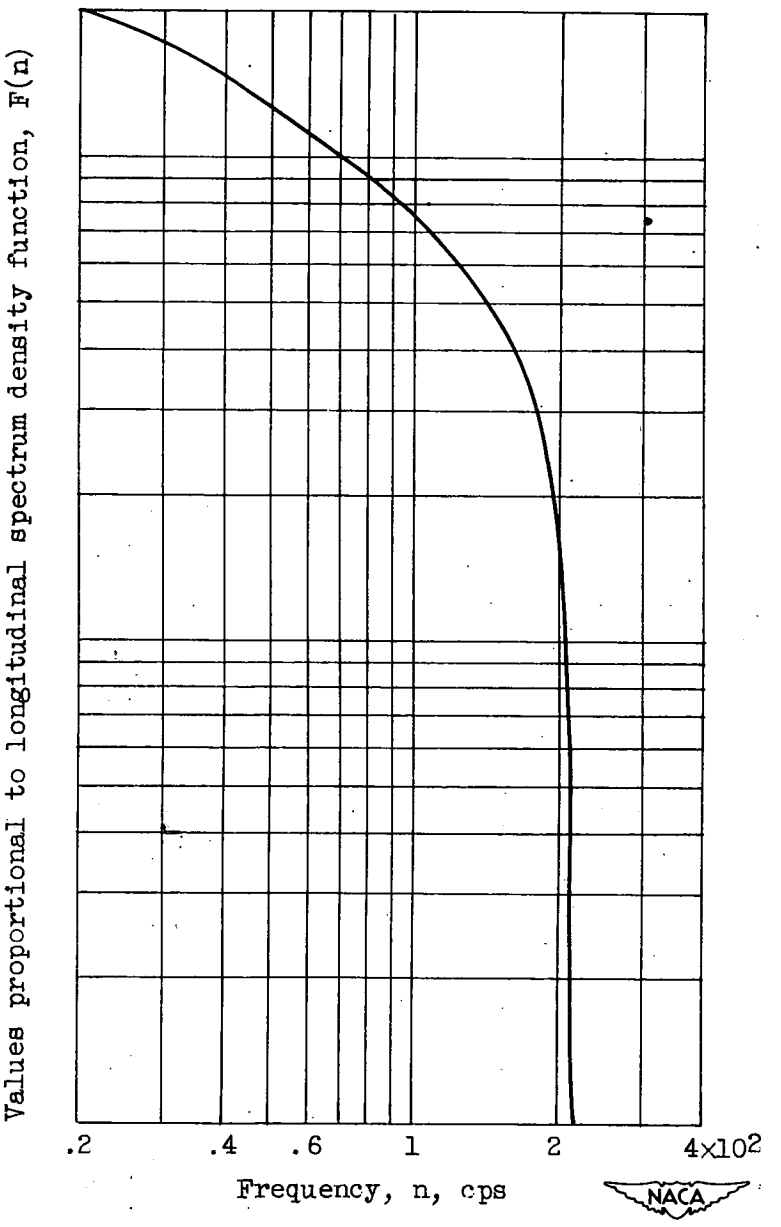

(b) Longitudinal velocity fluctuations originating in exhaust facilities.

Figure 10. - Continued. Measured longitudinal energy spectrum.

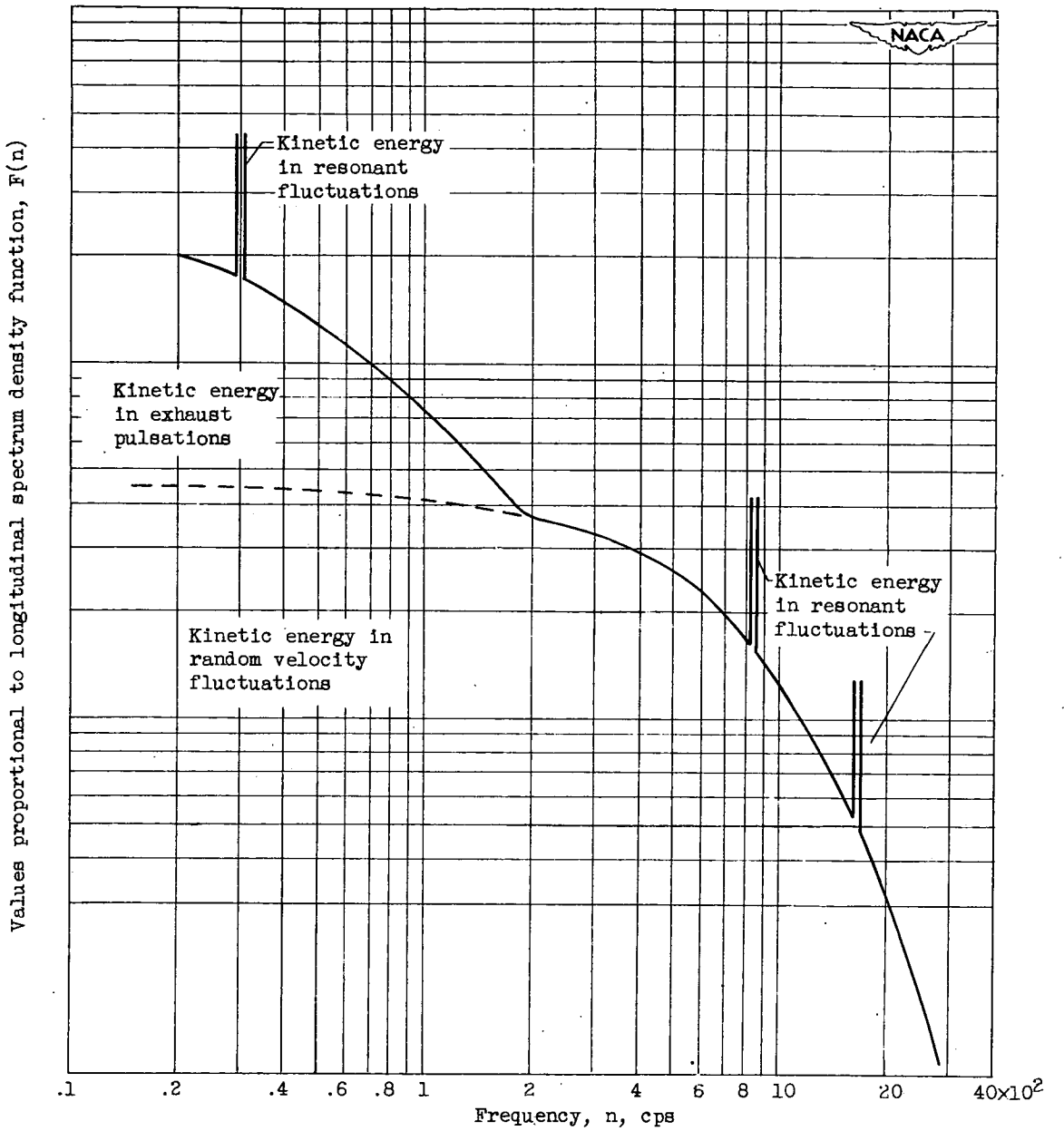

(c) Turbulence with superimposed exhaust pulsations and ducting resonance showing contribution of each to total spectrum. Mean stream velocity, 50 feet per second; stream static pressure, 5 inches of mercury absolute; air temperature, 540° R.

Figure 10. - Concluded. Measured longitudinal energy spectrum.

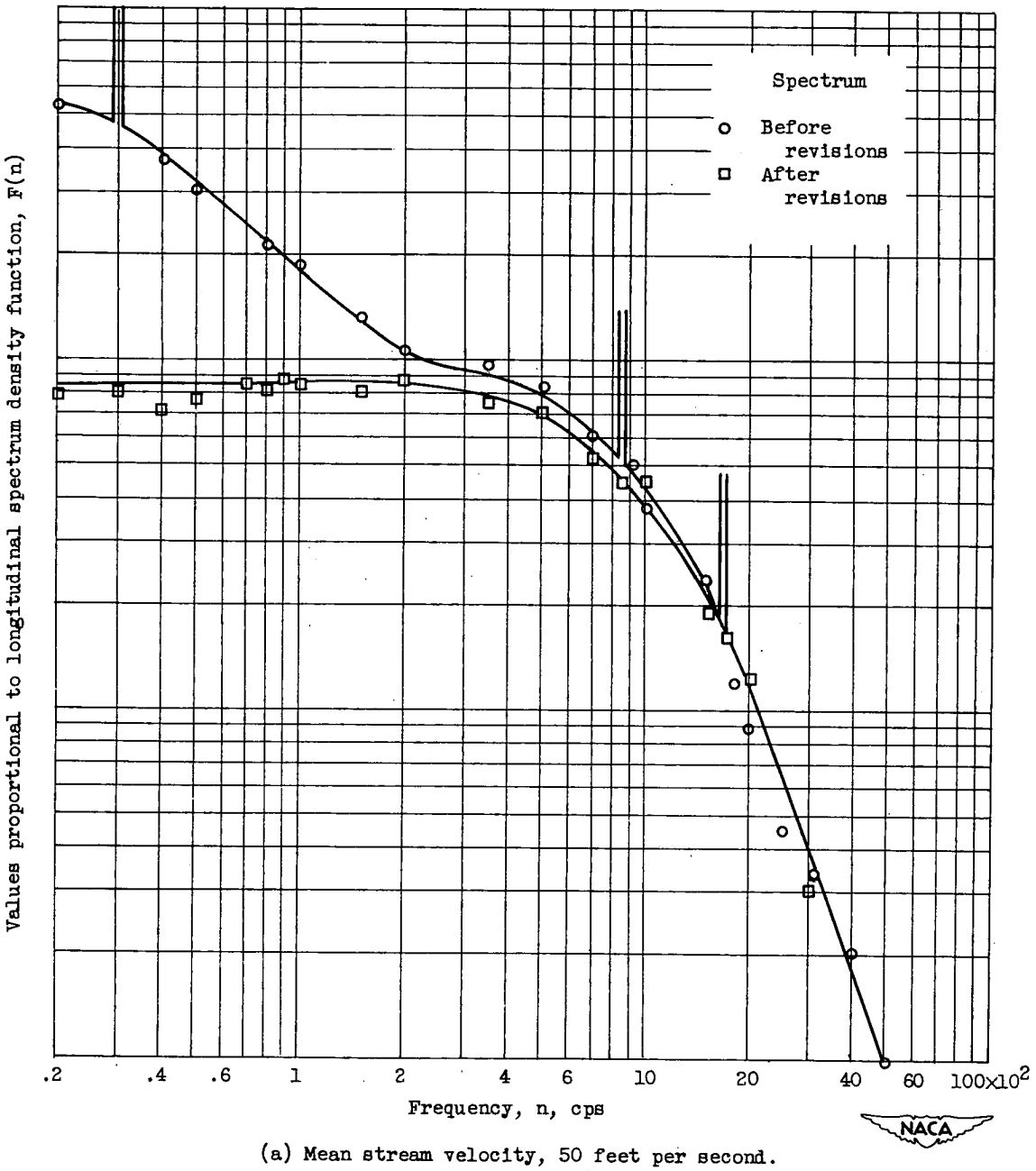

(a) Mean stream velocity, 50 feet per second.

Figure 11. - Longitudinal spectra before and after revisions of small-scale wind tunnel, 4.25 inches downstream of 0.045-inch-diameter by 0.225-inch mesh screen. Static pressure, 5 inches of mercury absolute; air temperature, 540° R.

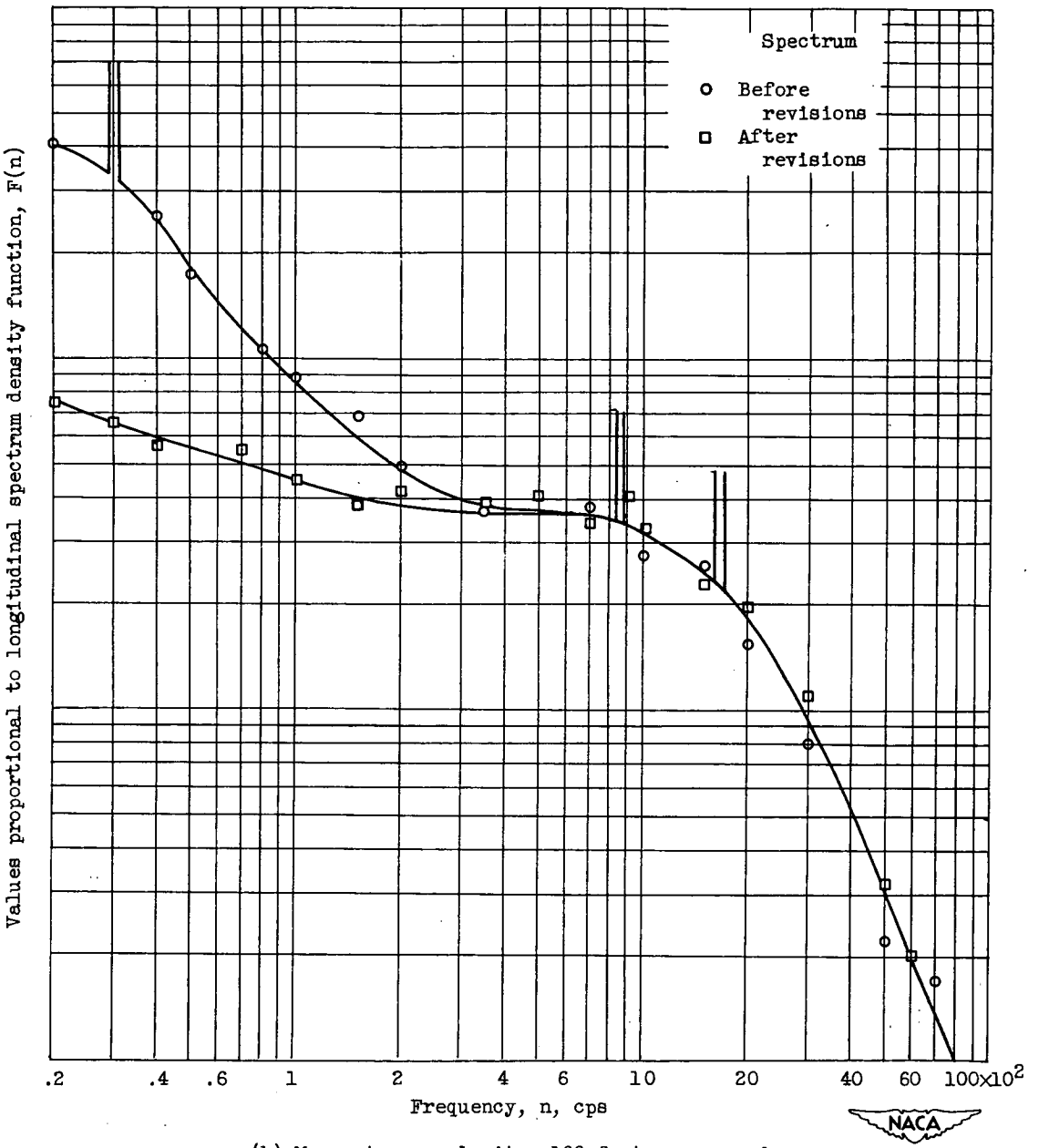

(b) Mean stream velocity, 100 feet per second.

Figure 11. - Continued. Longitudinal spectra before and after revisions of small-scale wind tunnel, 4.25 inches downstream of 0.045-inch-diameter by 0.225-inch mesh screen. Static pressure, 5 inches of mercury absolute; air temperature, 540° R.

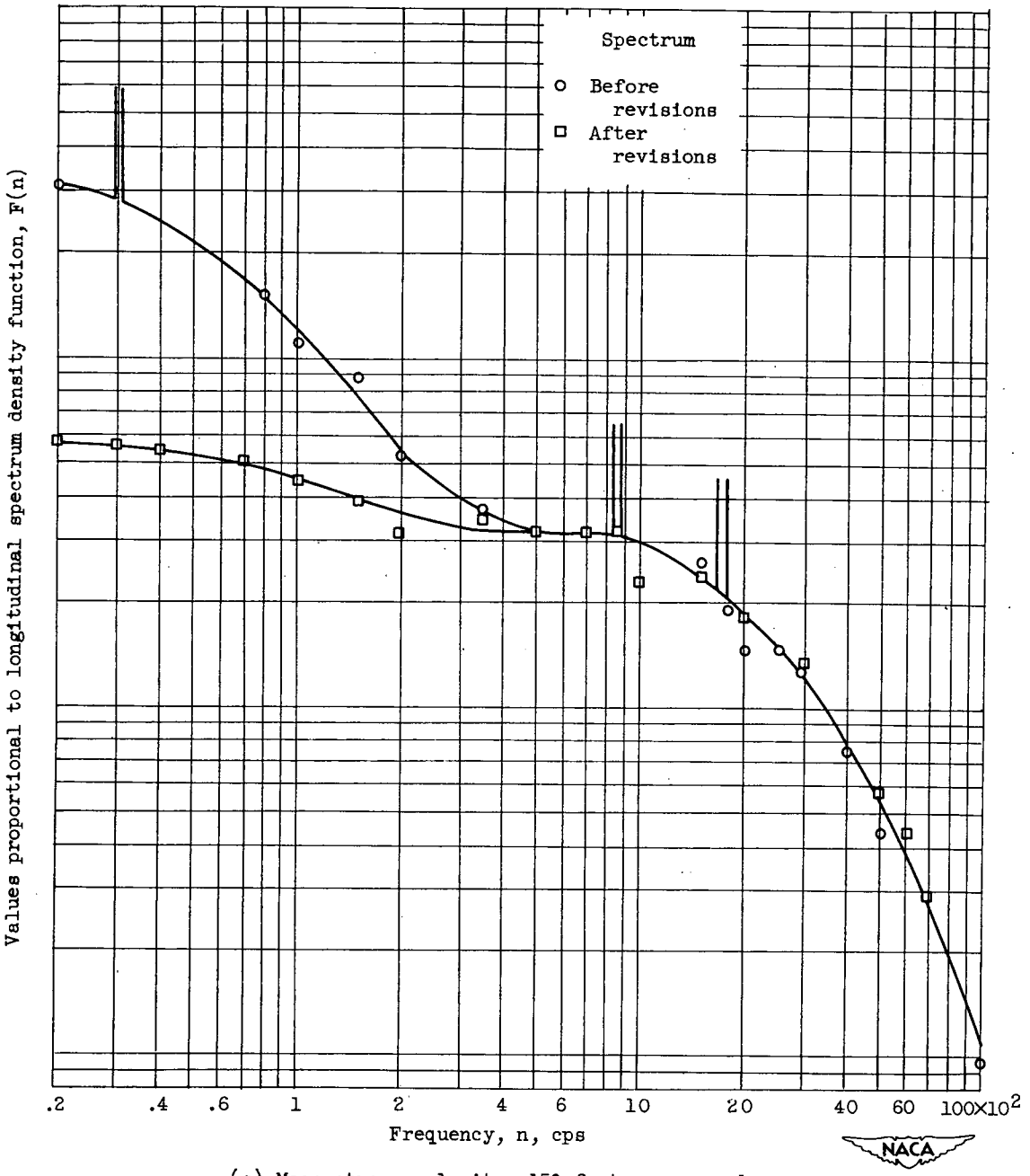

(c) Mean stream velocity, 150 feet per second.

Figure 11. - Continued. Longitudinal spectra before and after revisions of small scale wind tunnel, 4.25 inches downstream of 0.045-inch-diameter by 0.225-inch mesh screen. Static pressure, 5 inches of mercury absolute; air temperature, 540° R.

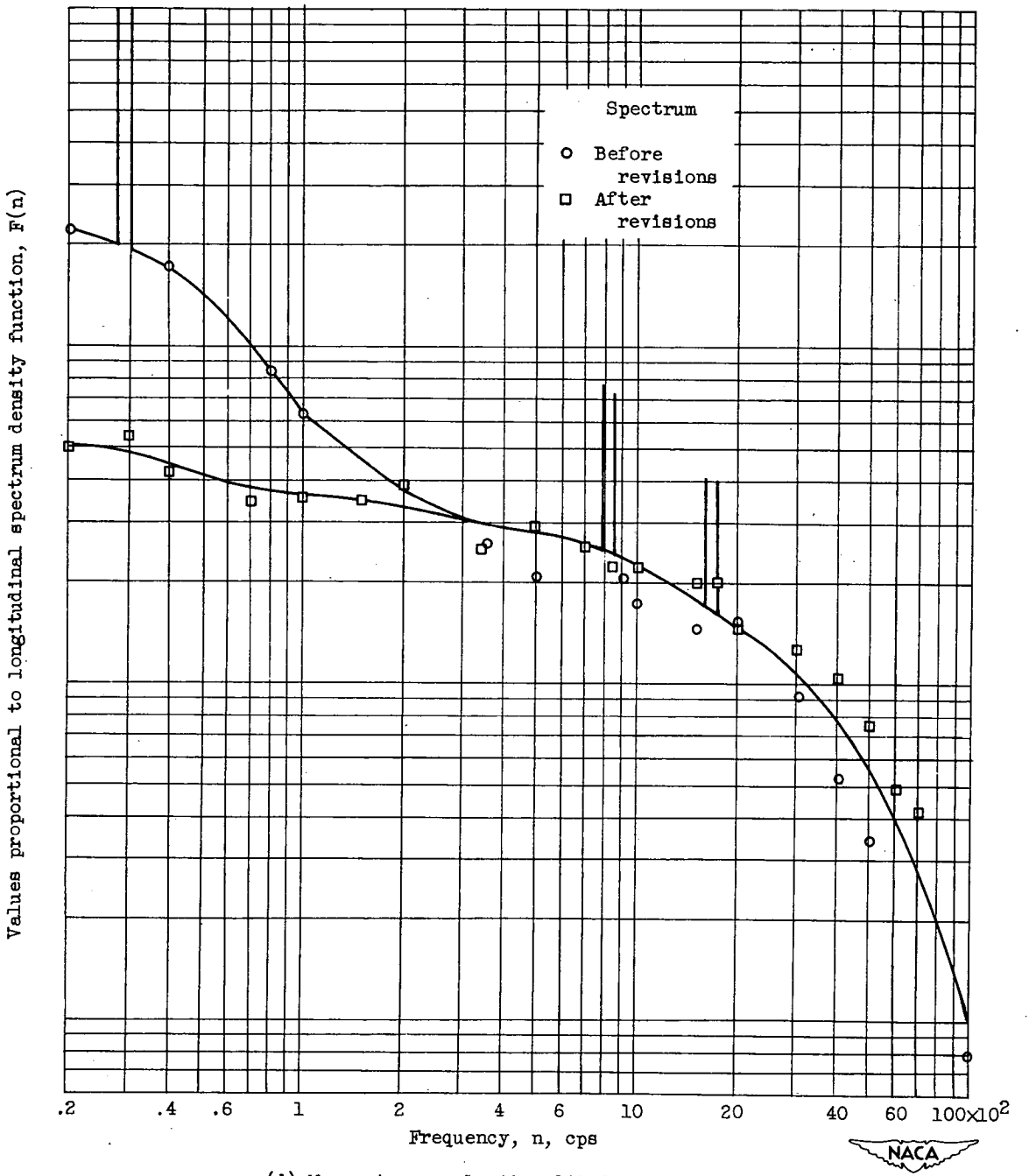

(d) Mean stream velocity, 200 feet per second.

Figure 11. - Continued. Longitudinal spectra before and after revisions of small-scale wind tunnel, 4.25 inches downstream of 0.045-inch-diameter by 0.225-inch mesh screen. Static pressure, 5 inches of mercury absolute; air temperature, 540° R.

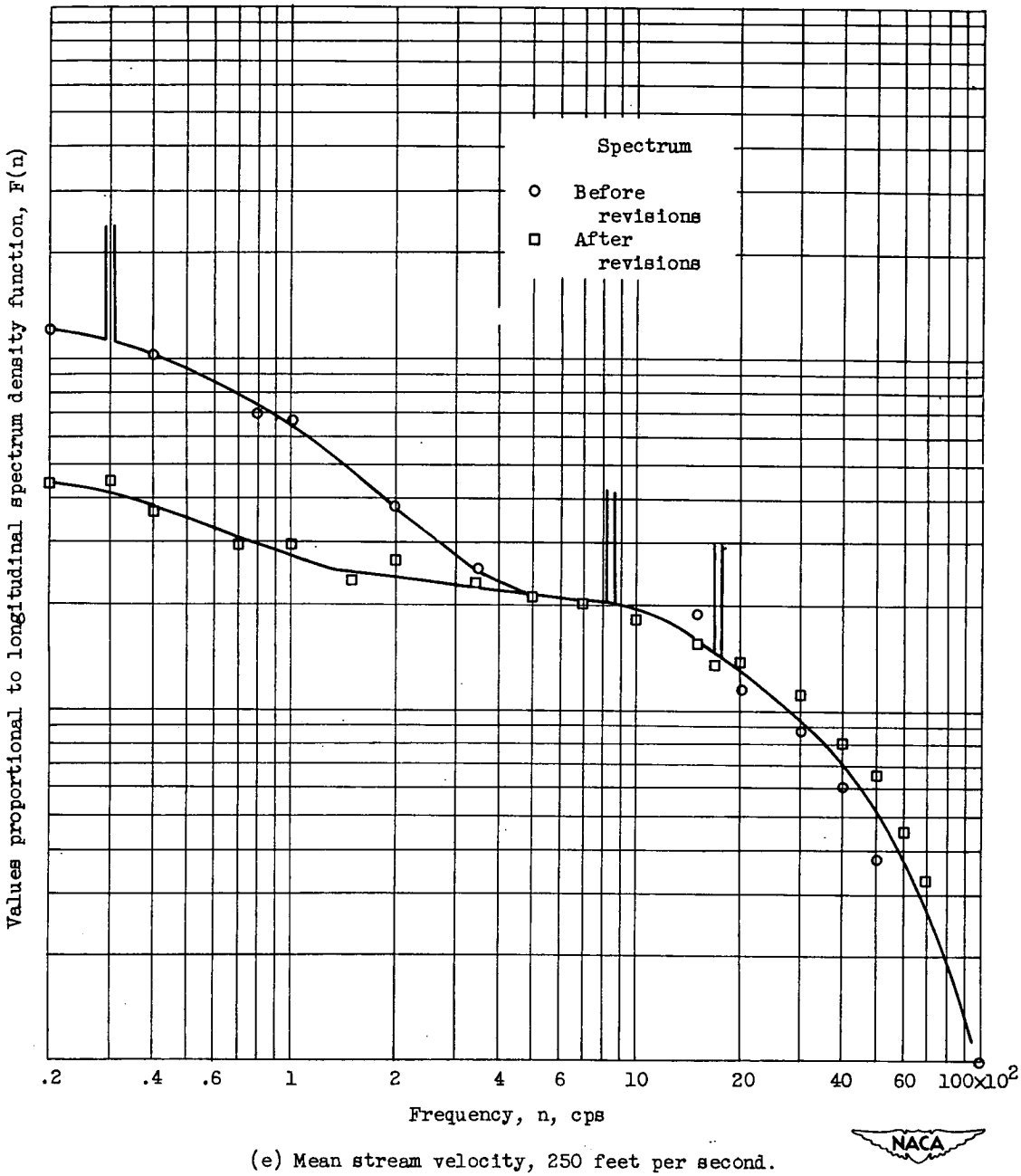

(e) Mean stream velocity, 250 feet per second.

Figure 11. - Concluded. Longitudinal spectra before and after revisions of small-scale wind tunnel, 4.25 inches downstream of 0.045-inch-diameter by 0.225-inch mesh screen. Static pressure, 5 inches of mercury absolute; air temperature, 540° R.

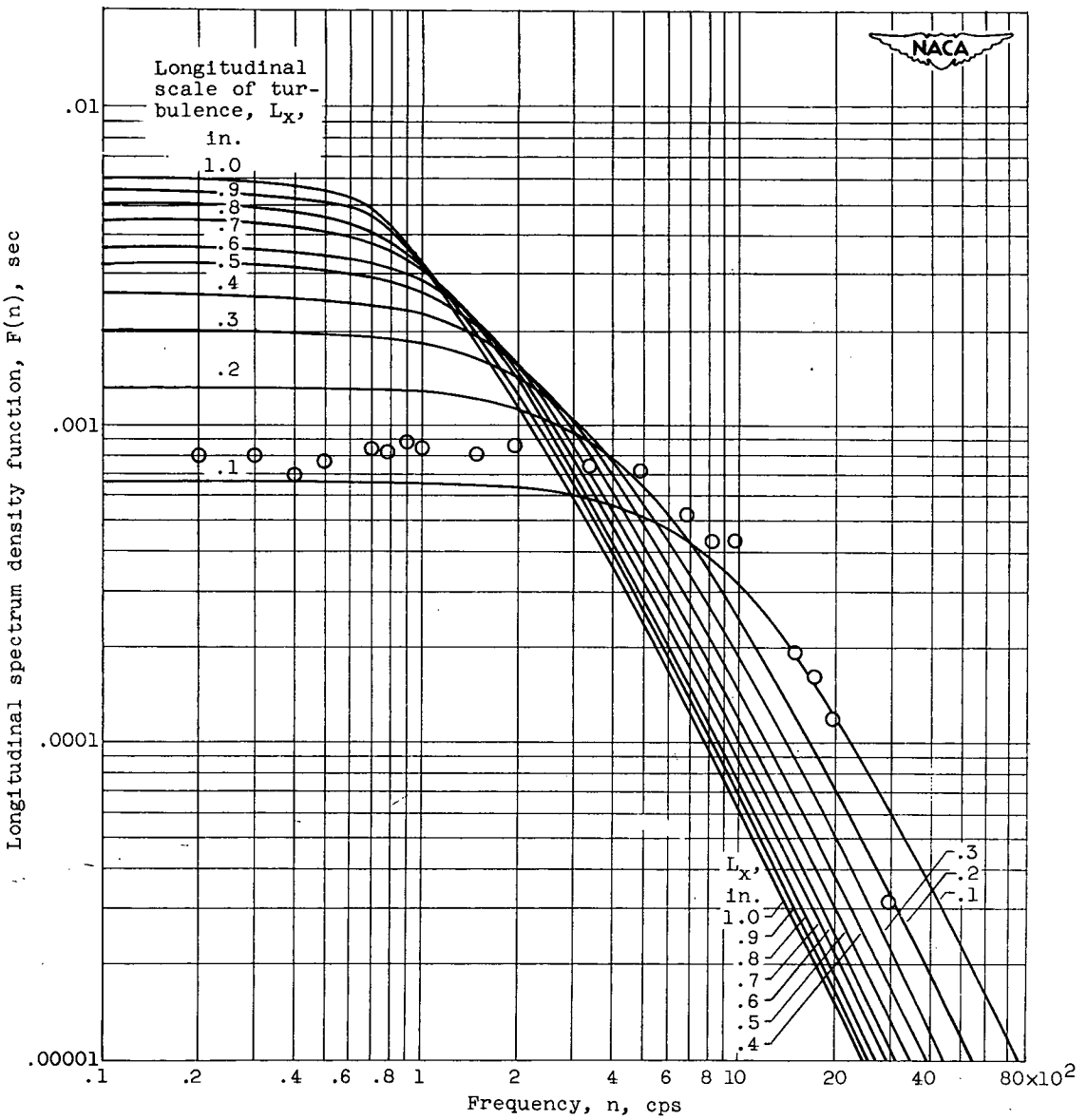

Figure 12. - Comparison of longitudinal spectrum measured in small-scale wind tunnel with theoretical longitudinal spectrum based on exponential form of longitudinal correlation coefficient. Mean stream velocity, 50 feet per second; stream static pressure, 5 inches of mercury absolute; air temperature, 540° R.

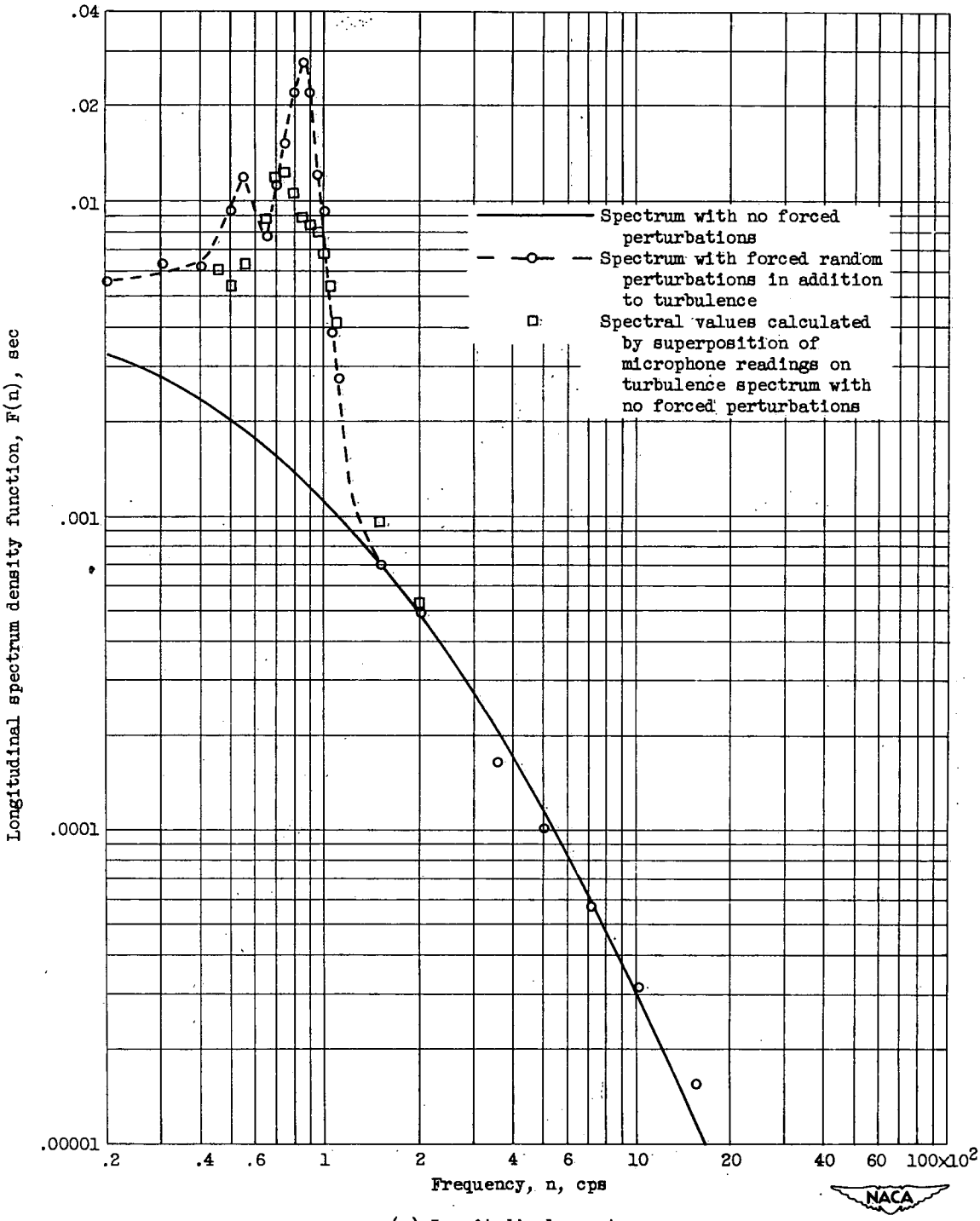

(a) Longitudinal spectra.

Figure 13. - Spectra of turbulence with and without forced random flow perturbations. Mean stream velocity, 50 feet per second; stream static pressure, 29 inches of mercury absolute; air temperature, 540° R.

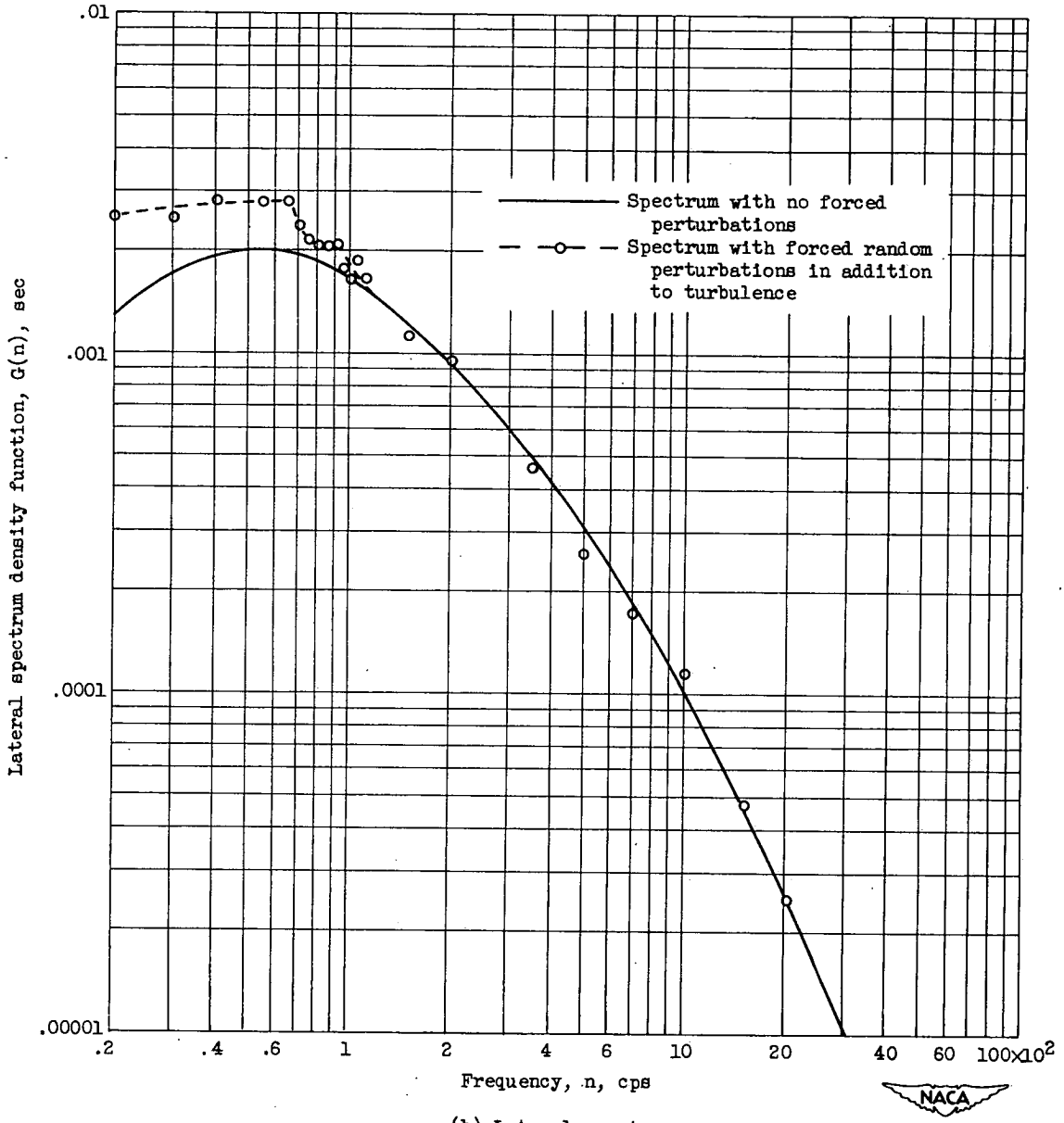

(b) Lateral spectra.

Figure 13. - Concluded. Spectra of turbulence with and without forced random flow perturbations. Mean stream velocity, 50 feet per second; stream static pressure, 29 inches of mercury absolute; air temperature, 540° R.

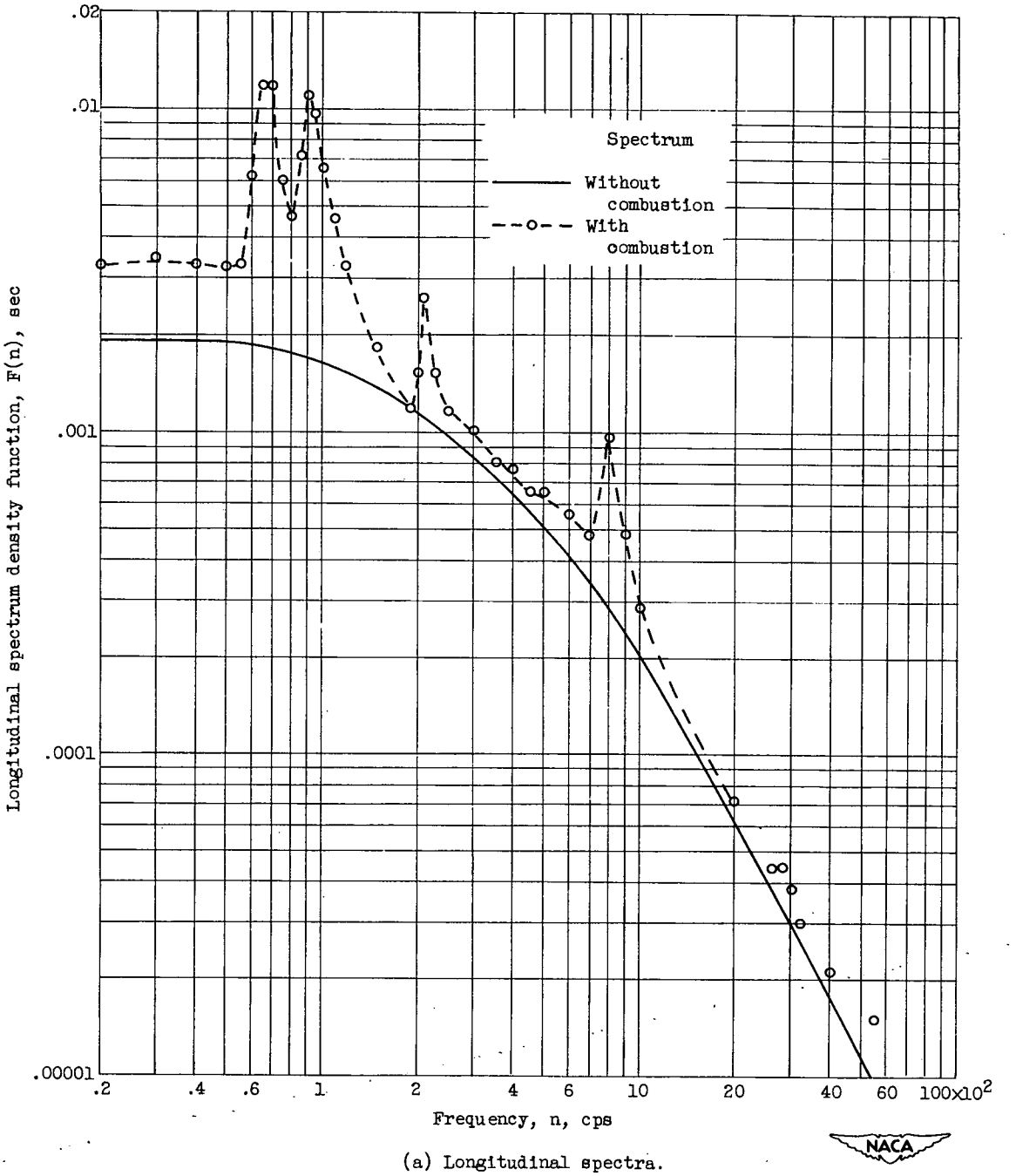

(a) Longitudinal spectra.

Figure 14. - Spectra in ram-jet test installation with and without combustion.

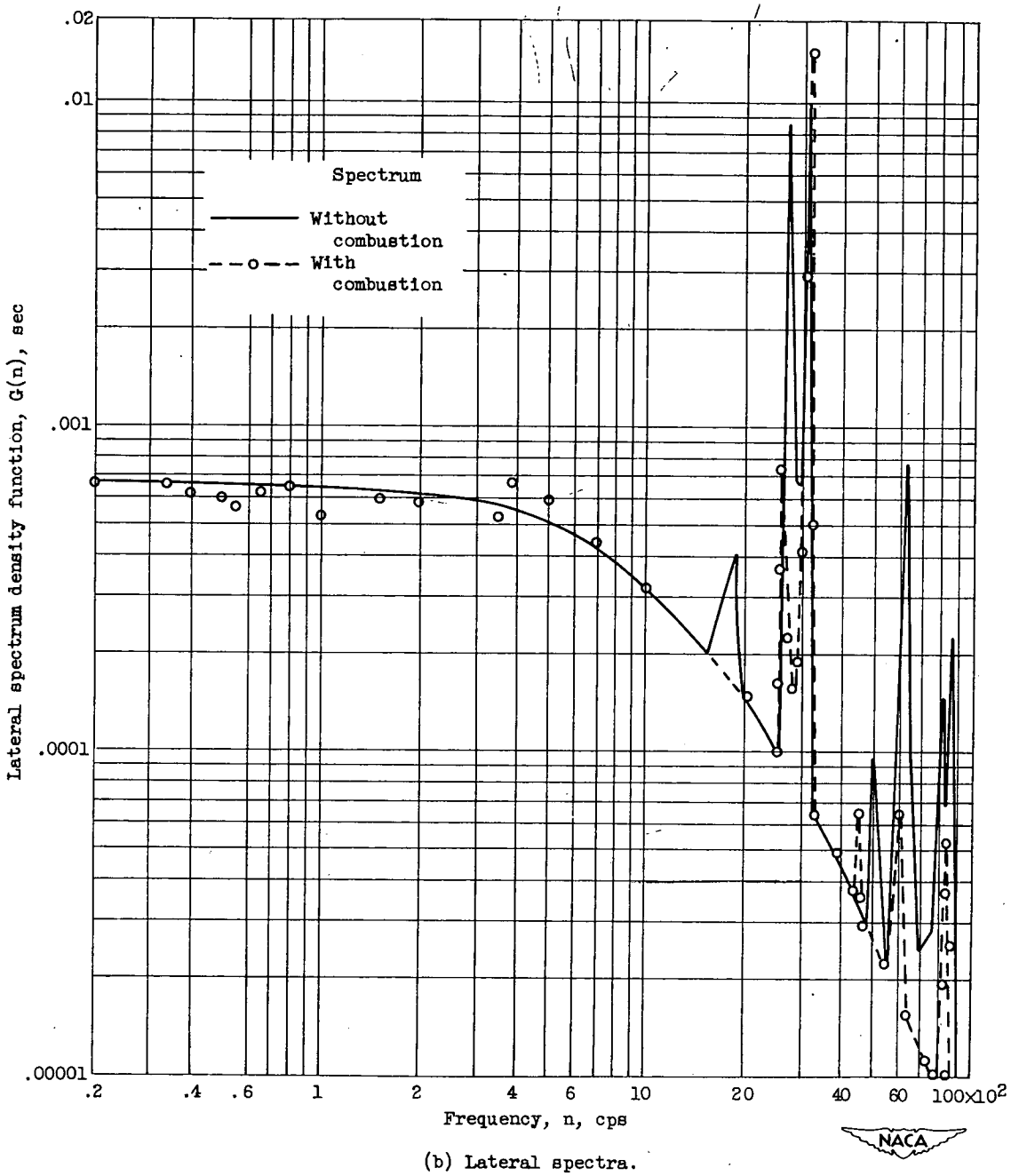

(b) Lateral spectra.

Figure 14. - Concluded. Spectra in ram-jet test installation with and without combustion.